THE ASTROPHYSICAL JOURNAL, 318:767–785, 1987 July 15

POWER SPECTRA OF QUASI-PERIODIC OSCILLATIONS IN LUMINOUS X-RAY STARS

N. SHIBAZAKI[1] AND F. K. LAMB[2]
Department of Physics, University of Illinois at Urbana-Champaign; and
Department of Physics and Center for Space Science and Astrophysics, Stanford University
Received 1986 July 16; accepted 1986 December 3

ABSTRACT

Quasi-periodic oscillations (QPOs) with frequencies in the range 5–50 Hz have recently been discovered in the intensity of more than half a dozen luminous X-ray stars. Random process models of the X-ray intensity time series provide a useful framework for analyzing the constraints imposed on physical models of QPO sources by measurements of the power-density spectra of their X-ray time series. Here we use this framework to study the effects on the power spectrum of several physical phenomena that may occur in the beat-frequency model.

One phenomenon is changes in the envelopes and oscillation wave forms of the X-ray pulses produced by density and magnetic-field fluctuations in the boundary layer. We show that the shape of the wave form can profoundly affect the strength of the oscillations relative to the red noise as well as the relative strengths of the harmonics of the oscillation frequency. We also demonstrate the effects on the power spectrum of distributions in the lifetimes and orbital frequencies of the fluctuations and present closed expressions that include these effects and are suitable for fitting to observed power spectral data.

Magnetospheric effects may impose nonuniform distributions of the times and initial stellar azimuths of the fluctuations. We illustrate the effects of nonuniform distributions of these quantities with some simple models. We show that variations in the rate of formation of fluctuations can produce peaks in the power spectrum at low frequencies where the red noise is strong. Interaction of the magnetosphere with persistent density patterns in the inner disk, fragmentation of larger scale fluctuations into smaller ones, and interaction between fluctuations may cause spatial clustering. We show that even very weak clustering can increase the strength of the oscillations relative to the red noise by one order of magnitude or more.

Although motivated by the beat-frequency model, our analysis of QPO power spectra in terms of random processes may be used to constrain a wide variety of physical models.

Subject headings: stars: accretion — stars: neutron — stars: X-rays — X-rays: binaries

I. INTRODUCTION

Relatively narrow peaks with centroid frequencies in the range 5–50 Hz have recently been discovered in power spectra of intensity time series from more than half a dozen very luminous X-ray stars, including GX 5−1 (van der Klis *et al.* 1985*a*, *b*; Elsner *et al.* 1986), Sco X-1 (Middleditch and Priedhorsky 1986; van der Klis and Jansen 1986; van der Klis *et al.* 1985*c*, 1986; Priedhorsky *et al.* 1986), Cyg X-2 (Hasinger *et al.* 1985, 1986; Norris and Wood 1985, 1986; Hasinger 1986*a*, *b*; Elsner *et al.* 1986), GX 3+1 (Lewin *et al.* 1986*a*, *b*), GX 17+2 (Stella, Parmar, and White 1985, 1987; Langmeier *et al.* 1985; Stella 1986), GX 349+2 (Lewin *et al.* 1985; Cooke, Stella, and Ponman 1985; Stella 1986), and 4U 1820−30 (Stella, White, and Priedhorsky 1985, 1987; Stella 1986). Possibly similar peaks have been reported at lower frequencies in the "rapid burster" (Tawara *et al.* 1982; Stella *et al.* 1985; Stella 1986), 4U 1626−67 (Joss, Avni, and Rappaport 1978; Li *et al.* 1980), Cyg X-3 (van der Klis and Jansen 1985), Terzan 2 (Belli *et al.* 1986), Cir X-1 (Tenant 1987), and GX 340+0 (van Paradijs *et al.* 1987).[3] These so-called quasi-periodic oscillations (QPOs) are often but not always observed in a given star. Even when observed, they are usually not readily apparent in the X-ray intensity time series. In the best-studied stars GX 5−1, Sco X-1, and Cyg X-2, the centroid frequency f_p of the principal peak is strongly correlated with the source intensity (see van der Klis 1986). The peaks typically have an area that corresponds to ~1%–10% rms variations in the X-ray intensity.

In most QPO sources, red noise is evident in the power spectrum at frequencies below f_p. In GX 5−1 and Cyg X-2 the total apparent power in the red noise[4] is comparable to or even greater than the total power in the oscillations. However, in Sco X-1, GX 17+2, and the "rapid burster" the total apparent power in the red noise appears to be much less than that in the oscillations. In GX 5−1, Sco X-1, and GX 17+2 red noise remains even when the oscillations are weak or absent.

The appearance of peaks in the power density spectra of these sources does not necessarily imply the existence of a harmonic or deterministic component in the X-ray intensity time series (see, for example, the discussion of random autoregressive processes by Scargle [1981]). However, most of the physical models so far proposed to account for the peaks

[1] Also at Space Science Laboratory, NASA/Marshall Space Flight Center.

[2] Also at Department of Astronomy, University of Illinois at Urbana-Champaign.

[3] Peaks have also been reported in power spectra of the optical and X-ray intensity from some cataclysmic variables. See Patterson (1979) and Cordova and Mason (1983).

[4] Here and below we use the phrase *total apparent power in the red noise* to refer to estimates of the total power in the red noise made by integrating over all frequencies an empirical expression for the power density motivated by the spectrum seen in the observed frequency band. Such estimates may of course differ from the actual total power in the red noise.

assume they are produced by a harmonic component of the X-ray intensity time series. Proposals include loops of magnetic flux in a strongly sheared boundary layer between the accretion disk and the surface of a slowly rotating nonmagnetic neutron star (Hameury, King, and Lasota 1985), oscillations in an X-ray–induced corona above the accretion disk (Boyle, Fabian, and Guilbert 1986), and shockwaves at the magnetospheric boundary of a weakly magnetic neutron star (Morfill and Trümper 1986). One model that appears particularly promising at present is the so-called beat-frequency modulated-accretion (BFMA) model (Alpar and Shaham 1985; Lamb *et al.* 1985, hereafter Paper I; Lamb 1986). In this model, the QPO sources are assumed to be weakly magnetic neutron stars accreting from Keplerian disks in which there are density and magnetic-field fluctuations. Interaction of the magnetosphere with the fluctuations in the inner disk causes the mass-accretion rate and hence the X-ray luminosity to vary at a harmonic of the beat frequency given by the difference between the frequency of revolution of the plasma in the magnetospheric boundary layer and the rotation frequency of the star.

The BFMA model appears attractive at present for several reasons. First, it makes a quantitative prediction of the QPO frequency. Second, the predicted frequency agrees with observed frequencies for neutron star rotation rates ~ 100 Hz and magnetic-field strengths $\sim 10^9$ G, values expected on the basis of earlier evolutionary arguments which suggest that the bright low-mass X-ray binaries are progenitors of the 100 Hz rotation-powered pulsars (see Alpar and Shaham 1985; van der Klis *et al.* 1985*b*; Paper I). Third, the narrowness of the QPO peaks is explained naturally by the narrowness of the magnetospheric boundary layer (Ghosh and Lamb 1979). Fourth, the variation of the beat frequency and source luminosity with mass accretion rate elegantly account for the observed variations of QPO frequency with accretion rate (Alpar and Shaham 1985; van der Klis *et al.* 1985*b*; Paper I; Priedhorsky 1986). Fifth, the model easily produces intensity variations at the QPO frequency comparable to the 5%–10% rms fractional variations observed (Paper I; Lamb 1986). Sixth, the model predicts that the oscillations and red noise should be most prominent in the (relatively hard) spectral component that comes from the neutron star (Paper I), in agreement with recent observational results (Hasinger 1986*b*; Priedhorsky *et al.* 1986; van der Klis *et al.* 1986; Lewin *et al.* 1986*b*). Seventh, the small magnetosphere, relatively weak surface magnetic field, and thick inner disk of the beat frequency model provide an explanation of the profound observed differences between the QPO sources and accretion-powered pulsars, including the fact that pulsations at the spin frequency are weak or absent in the former and strong in the latter (Paper I; Lamb 1986; Brainerd and Lamb 1987). Finally, the model provides a clear conceptual framework for developing quantitative models of the X-ray intensity time series and power spectra observed in the QPO sources.

If QPOs arise in the manner suggested by the BFMA model, the variation of the peak frequency with X-ray intensity depends on the spin rate and magnetic field of the neutron star and the gross properties of the mass and energy flows near the star, while the detailed shape of the spectrum, including the characteristics of the red noise and the shape of the oscillation peak or peaks, provides information about the physical processes taking place in the boundary layer between the disk and the magnetosphere and the properties of the accretion flow within the magnetosphere. Thus, if the BFMA model proves correct, quasi-periodic oscillations in bright X-ray stars are an extremely valuable probe of the boundary layers and magnetospheres of weakly magnetic neutron stars.

As explained in Paper I, the X-ray intensity time series predicted by the BFMA model can be represented mathematically by a random process. This is because each fluctuation in the boundary layer may be regarded as giving rise to a disturbance of the X-ray intensity that lasts only for a finite time and has a component that varies at the beat frequency. The expected properties of the X-ray time series and the power-density spectrum produced by a sequence of such pulses may then be calculated using the theory of random processes, making possible a quantitative analysis of the constraints imposed on the physical model by the available observations.[5]

The random process analysis of Paper I showed that the strengths of the oscillations relative to the red noise are inconsistent with *any* physical model in which disturbances of the X-ray emission are uncorrelated, have a sinusoidal wave form with nonzero mean, and persist only for a finite time (see also Lamb 1986). This conclusion has been strengthened by subsequent observational results, including the extension of power spectral observations of Sco X-1 to frequencies as low as 0.016 Hz (Priedhorsky *et al.* 1986) and estimates of the apparent total power in the red noise that are at least one order of magnitude smaller than the power in the oscillations (van der Klis and Jansen 1986; Priedhorsky *et al.* 1986; van der Klis *et al.* 1986). Paper I pointed out that several physical phenomena, including nonsinusoidal pulse wave forms, broad distributions of pulse lifetimes extending to relatively long times, and correlations between pulses, could generate power spectra consistent with the observations then available. In the present paper we use random process models to study the effects of these and other phenomena that may occur in the beat-frequency model, comparing the power spectra they generate with current observational results.

We show that the shape and mean value of the oscillating component of the X-ray pulse wave form profoundly affect the strength of the oscillations relative to the red noise. We also explore the effects on the power spectrum of distributions in the lifetimes and orbital frequencies of the fluctuations in the boundary layer and show that the lifetime distribution, especially, can strongly affect the red-noise spectrum. We present closed expressions that include these effects and are suitable for fitting to observed power spectral data. Interaction of the magnetosphere with persistent density patterns in the inner disk, fragmentation of larger scale fluctuations into smaller ones, and interaction between fluctuations may cause some of the fluctuations to be clustered. We show that even very weak spatial clustering can cause the total power in the oscillations to exceed that in the red noise by a large factor. We demonstrate that these phenomena can account for the power spectra observed to date. Moreover, changes in the wave forms of pulses, the lifetimes of fluctuations, and the degree of clustering can produce complex relationships between the properties of the red noise and the oscillations, as noted in Paper I.

Finally, we consider some simple models that illustrate the effects on the power spectrum of nonuniform distributions of

[5] Here and below we use the term *pulse* to refer to a single event of finite duration that disturbs the X-ray intensity. This usage is consistent with the existing literature on random processes (see, for example, the review by Scargle [1981]). Individual pulse wave forms *may* have a periodic component. Our use here of the term pulse does *not* imply *periodic* pulsation.

the initial stellar azimuths and times of the fluctuations, which could be caused by their interaction with the magnetospheric field and plasma. We show also that variations in the rate of formation of fluctuations can produce peaks in the power spectrum and that peaks caused by such variations can be discriminated from peaks formed by oscillations in the pulse wave forms. Peaks caused by variations in the pulse rate are strongest and hence most readily observed at low frequencies, where the red noise is strong.

Although motivated by the BFMA model, our results have much wider applicability since, as pointed out by Lamb (1986), random processes can also be used to describe the X-ray intensity time series predicted by a variety of other QPO models. Therefore, in the following sections we make clear the types of physical models which give time series that can be represented by the random processes we consider.

The remainder of the paper is organized as follows. In § II we summarize the relevant physical properties of the beat-frequency model and introduce the class of random processes we shall use to represent the X-ray intensity time series predicted by this model. We also note the conditions required for the X-ray flux given by other physical models to be represented by this class of random processes and introduce the relatively simple *reference* power spectrum to which we compare the more complicated spectra computed in later sections. In § III we discuss the dependence of the power-density spectrum on pulse shape. We introduce pulse-lifetime and orbital-frequency distributions and illustrate how these affect the power density spectrum in § IV. In § V we consider the effect of nonuniform initial-pulse-phase distributions and in § VI, nonuniform pulse-time distributions. In § VII we analyze the effect of a particular type of pulse-to-pulse correlation that may be natural in the context of the BFMA model and that greatly increases the power in the oscillations relative to that in the red noise. Readers not interested in the details of our calculations may turn directly to § VIII, where we summarize our results, compare them with current data, and suggest possibly fruitful new observations. Our conclusions are summarized in § IX.

II. MODELS

In this section we first summarize the relevant physical properties of the beat-frequency modulated-accretion model and then introduce the class of random processes we shall use to represent the X-ray intensity time series predicted by this model. We also introduce the relatively simple reference power spectrum to which we shall compare the more complex spectra of some later sections and give general expressions for the total power in the red noise and QPO peaks that we shall need later.

a) Physical Model

In the BFMA model, the QPO sources are assumed to be weakly magnetic neutron stars accreting from Keplerian disks at rates close to the Eddington critical rate. Because of the weak magnetic field and high accretion rate, the narrow boundary layer where the magnetosphere interacts strongly with the disk (Ghosh and Lamb 1979) lies at most a few stellar radii from the surface of the star. As indicated in Paper I, several physical mechanisms are expected to produce density and magnetic field fluctuations in the inner disk and the boundary layer. These include the Kelvin-Helmholtz instability, thermal instabilities, and the so-called Parker instability. As a result of these mechanisms, the plasma in the boundary layer is expected to be spatially inhomogeneous, either because fluctuations are carried into the boundary layer from the inner disk or because they occur within the boundary layer.

Consider first interaction of the magnetospheric field and plasma with fluctuations in which the plasma density is higher than average. The motion of such clumps through the magnetosphere causes plasma to be stripped from them by the stresses exerted on their surfaces and by reconnection of their magnetic fields to the magnetospheric field. Once stripped from such clumps, plasma is quickly brought into corotation with the neutron star and accretes to the stellar surface, producing X-rays. Unless the magnetic field is axisymmetrical, aligned with the rotation axes of disk and star, and centered in the star, a given clump interacts with the magnetosphere more strongly at some stellar azimuths than at others. As a result, plasma is stripped from the clump at a higher rate at some azimuths than at others.

The variation of the stripping rate with stellar azimuth causes the mass flux to the stellar surface contributed by the clump to vary periodically at one or more harmonics of the frequency with which the fluctuation moves around the magnetosphere. This variation will occur at the fundamental if the stripping rate increases and decreases only once per circuit, or at an overtone if more than once. The frequency with which a given clump moves around the star is just the beat frequency ω_B given by the difference between the orbital frequency Ω_c of the clump and the rotation frequency Ω_s of the star, that is,

$$\omega_B = \Omega_c - \Omega_s \,. \tag{1}$$

We expect Ω_c to be $\approx \Omega_K(r)$, the Keplerian frequency at the radius r of the clump. As discussed in Paper I, the widths Δf_p of the principal oscillation peaks observed in several sources are consistent with this expectation.

If the existence of other density and magnetic-field fluctuations does not affect the stripping process, the disturbance in the mass flux from the boundary layer to the stellar surface produced by a single clump is just the mass flux stripped from the clump and hence is always positive. Even if the fluctuations within the boundary layer are randomly distributed in stellar azimuth (see Fig. 1), there will always be a slight excess at some azimuth, causing the mass flux from the boundary layer and hence the X-ray luminosity of the star to vary at the frequency ω_B.

The interaction of the magnetospheric field and plasma with a fluctuation in which the plasma density is *less than average* is similar, except that the disturbance in the mass flux to the stellar surface and hence the disturbance in the X-ray intensity produced by such a void is negative. However, the amplitude of such voids and their distribution in space is constrained by the fact that the plasma density in the boundary layer cannot be negative. When this local constraint is applied to all parts of the boundary layer, it guarantees that the intensity, which reflects accretion of plasma from the entire layer, is positive. The result of a random distribution of both clumps and voids is again a mass flux to the stellar surface that varies periodically at one or more harmonics of the beat frequency.

In reality, the variation of the magnetospheric field with stellar azimuth is likely to impose nonrandom variations of the properties of the fluctuations. Also, interactions between fluctuations are likely to produce correlations in their rates of occurrence, positions, and other properties. If, for example, the presence of a given density fluctuation affects other fluctuations, the structure of the magnetosphere, and the stripping rate, then the disturbance of the mass flux and the X-ray lumin-

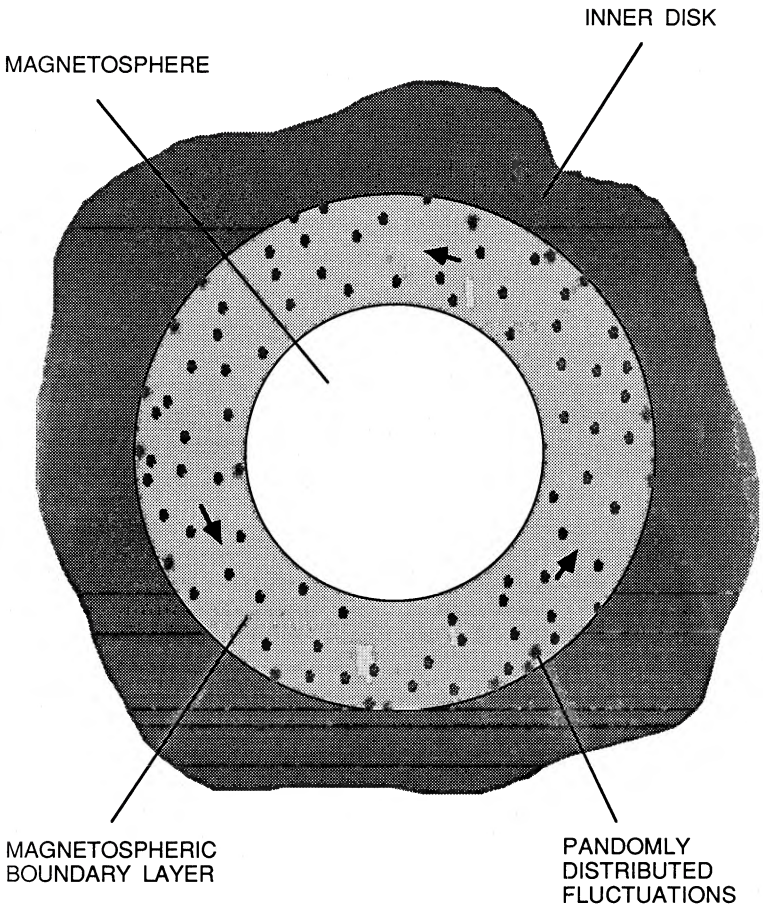

FIG. 1.—Top view of the narrow boundary layer at the inner edge of the disk from which plasma flows to the surface of the neutron star, showing a random distribution of density fluctuations. In the frame of the star, a given fluctuation moves with azimuthal velocity $r\omega_B(r)$ and radial velocity v_r.

osity caused by the given clump (void) need not be positive (negative) at all times, since enhanced accretion from one stellar azimuth may suppress accretion from another, and vice versa. If so, the mean value of the X-ray pulses produced by fluctuations may be reduced. In principle, the mean value of the pulses could even be zero, if clumps cause voids on the opposite side of the magnetosphere and vice versa.

Several mechanisms may cause fluctuations in the boundary layer to be spatially clustered. For example, interaction of the magnetosphere with persistent density variations in the inner disk (see Zurek and Benz 1986) may cause density fluctuations to enter the boundary layer at more or less random times but at the azimuths of the density variations in the inner disk, producing spatial clustering of fluctuations in the boundary layer. Interaction of the magnetosphere with larger fluctuations in the inner disk may cause them to fragment into smaller but more numerous fluctuations that are spatially clustered. If the existence of a slight local excess of plasma orbiting in the boundary layer enhances the rate at which plasma in the inner disk enters the boundary layer at the azimuth of the excess, variations in density within the boundary layer will persist. Finally, interaction between fluctuations within the boundary layer may cause them to cluster. If any of these mechanisms operate, there will be some spatial clustering of fluctuations within the boundary layer, as shown in Figure 2.

b) Random Process Model

The physical picture just described suggests that the X-ray intensity time series $I(t)$ of the source can be represented as a series of pulses, each describing the disturbance of the mean X-ray intensity caused by a single density fluctuation in the boundary layer in the presence of other fluctuations. We shall assume that a single realization of the time series may be written as a superposition of the disturbances of the intensity caused by the individual fluctuations, that is,

$$I(t) = I_0 + \sum_{i=-\infty}^{\infty} F(t - t_i) , \qquad (2)$$

where I_0 is a possible constant intensity produced by emission from the disk or accretion to the star of plasma not in fluctuations, F is the wave form of the disturbance of the X-ray intensity produced by a single fluctuation, and t_i is the time of the X-ray pulse produced by the ith fluctuation. In order to be physical, $I(t)$ must be positive at all times. As noted above, this is guaranteed in the BFMA model by the fact that the inward mass flux from the boundary layer is positive.

Our assumption that the X-ray intensity time series can be represented by a superposition of pulses still allows us to take into account interactions between the fluctuations and the magnetosphere as well as any interactions between the fluctuations themselves that can be described in terms of pulse-to-pulse correlations of the times, initial phases, and other properties of the individual pulses $F(t)$. Other types of interactions between the fluctuations, for example, interactions that would require a multiplication of the individual pulse wave forms, cannot be described by a time series of this form. However, interactions between fluctuations described by multiplication of pulse wave forms would produce sidebands,

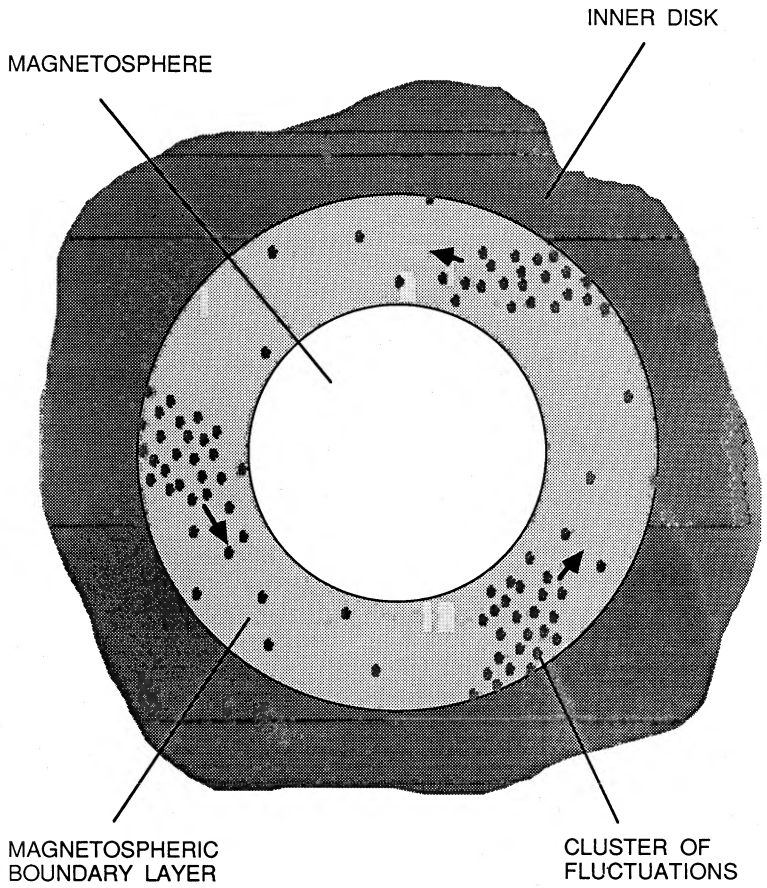

FIG. 2.—View as in Fig. 1, illustrating spatial clustering of density fluctuations caused, for example, by fragmentation of larger fluctuations into smaller ones as fluctuations drift from the inner disk into the boundary layer.

even if the beat frequencies of all the fluctuations were the same. Thus, for a large number of fluctuations the power in the oscillations would be spread over a large number of sidebands, producing a broad excess of power rather than a single, well-defined peak. While this type of interaction may be relevant to QPO spectra in which the oscillation peak is very broad, it will not be considered further in the present paper.

Any arbitrary pulse wave form $F(t)$ can be expressed as a harmonic series in the frequencies f_n, where $f_n = n/\tau$ in terms of the duration τ of the pulse. However, one aspect of the BFMA model is that it suggests a particular class of pulse shapes. On physical grounds, one may expect that the disturbance of the X-ray intensity caused by a single fluctuation will increase and decrease over the lifetime τ of the fluctuation, and that the disturbance will have components that oscillate at one or more harmonics of the beat frequency $f_B = \omega_B/2\pi$. Harmonics of f_B may appear either because the interaction between a fluctuation and the magnetosphere varies more than once per circuit around the magnetosphere or because the oscillating component of the pulse wave form produced by the interaction does not have a purely sinusoidal shape, or both.

To the extent that each fluctuation within the boundary layer drifts radially inward, its orbital frequency, and hence the beat frequency corresponding to it, will increase slightly during its lifetime. As discussed further in § VIII, unless the change Δf_B in the beat frequency is large compared to $1/\tau$, this increase in f_B only produces small-amplitude wiggles in the wings of the oscillation peak. Since fits of model power spectra to observed power spectra indicate that Δf_B is not large compared to $1/\tau$, and since we wish to focus in this paper on important questions concerning the large-scale features of the power spectrum, we shall take f_B to be constant in time.

Motivated by these considerations, we assume the pulse $F(t)$ may be written as the product of an *envelope function* $G(t)$ that describes the rise and fall of the pulse and a *modulation function* $H(t)$ that describes the variation of the pulse wave form at f_B and its overtones, that is,

$$F(t) = G(t)H(t) , \tag{3}$$

where $G(t)$ is positive and normalized according to

$$\int_0^\infty G(t)dt = \tau \tag{4}$$

and

$$H(t) = A + \sum_{n=1}^{\infty} B_n \cos\left[n(2\pi f_B t + \phi) + \alpha_n\right] . \tag{5}$$

Here t is measured *from the origin of time of the pulse*, ϕ is the pulse phase at $t = 0$, and α_n is the relative phase of the nth harmonic in the pulse wave form. The initial phase ϕ is equal to the initial stellar azimuth of the fluctuation that produces the pulse. The values of the variables τ, A, B_n, f_B, ϕ, and α_n in the ith pulse in the series (2) will be denoted by the subscript i. We assume that the values of these variables in a collection of pulses are distributed according to probability densities to be specified. Of particular interest to us are situations in which some of these variables are correlated.

If all fluctuations are increases in density and the only disturbance of the X-ray intensity is that produced by the mass flux to the stellar surface contributed by accretion from such fluctuations, all pulses $F(t)$ and hence all modulation functions $H(t)$ must be positive at all times. On the other hand, if some fluctuations are decreases in density or if accretion of plasma from one azimuth suppresses accretion from another, some modulation functions may be negative all or part of the time. The distributions of the parameters in $H(t)$ and the distribution of pulses in time are then constrained by the requirement that $I(t)$ have zero probability of becoming negative. Even if some disturbances $F(t)$ are positive at some times and negative at others, most wave forms will not have zero mean [i.e., A_i in $H(t)$ will not be zero] unless some mechanism acts to "tune" the wave forms to have zero mean.

The key assumptions incorporated in equations (2)–(5) are (*a*) the X-ray intensity time series may be expressed as a constant intensity plus a sum of pulses, (*b*) the shapes of the pulses may be expressed as harmonic series in the pulse phase, (*c*) the increase in pulse phase is proportional to $f_B t$, where f_B is some basic frequency that can be treated as constant in time.

c) *Reference Spectrum*

In the following sections it will be helpful to have a relatively simple power-density spectrum with which to compare the more complex spectra derived there. For this purpose we shall use the power-density spectrum of the X-ray intensity time series (2) that results if the pulse times t_i and initial phases ϕ_i are uncorrelated and uniformly distributed, and if the distributions of A, B_n, α_n, f_B, and τ are uncorrelated and independent of time. Uniform distributions of t_i and ϕ_i are appropriate if the fluctuations enter the boundary layer or form within it at completely random times and at completely random stellar azimuths. The resulting *reference spectrum* may be written (cf. Paper I and Rice 1954)

$$\langle P(f)\rangle_{\rm ref} = 2\langle I\rangle^2\delta(f) + 2\langle I\rangle + 2\nu\langle A^2\rangle|S(f)|^2 + \frac{\nu}{2}\sum_{n=1}^{\infty}\langle B_n^2\rangle[|S(f-nf_B)|^2 + |S(f+nf_B)|^2], \quad (6)$$

where ν is the pulse rate and $S(f)$ is the Fourier transform of the envelope function $G(t)$. The angle brackets in equation (6) denote an average over an ensemble of realizations of the time series (2). The assumption that t_i is uniformly distributed implies that ν is independent of time. Because all distributions have been assumed time-independent, the average of the intensity over a long time interval is equal to the average $\langle I\rangle$ of the intensity over an ensemble of time series. Furthermore, $\langle I\rangle = I_0 + \langle N\rangle\langle A\rangle$, where $\langle N\rangle = \nu\tau$ is the mean number of pulses in time τ.

The terms on the right side of equation (6) may be interpreted as follows. The first term is the power at zero frequency arising from the nonzero mean intensity. The second term describes the power density of the Poisson noise due to photon counting statistics whereas the third term, proportional to $|S(f)|^2$, represents the power density of the excess noise caused by variations in the photon arrival rate produced by the nonzero means of some pulses. The power density of this latter component of the spectrum is almost constant at frequencies $f \ll 1/2\pi\tau$ but rolls off at higher frequencies, giving a red spectrum. We therefore refer to it below as the *red-noise* component. The terms proportional to $|S(f-nf_B)|^2$ describe the power density near f_B and its overtones produced by any oscillating components in the pulse wave form. The terms proportional to $|S(f+nf_B)|^2$ can be neglected for most envelope functions of interest. The function $S(f)$ includes the "lifetime" broadening (HWHM $\Delta f_L = 1/2\pi\tau$) produced by the finite duration τ of each pulse. Note that the shape of the red-noise spectrum is the same as the shape of the wings of the oscillation peaks.

For the reference spectrum, the *total* power in the zero-frequency, red noise, and various oscillating components is

$$P_0 = \int_0^{0+\epsilon}\langle P(f)\rangle df, \quad (7)$$

$$P_{\rm RN} = 2\nu\langle A^2\rangle\int_0^{\infty}|S(f)|^2 df, \quad (8)$$

and

$$P_n = \tfrac{1}{2}\nu\langle B_n^2\rangle\int_0^{\infty}|S(f-nf_B)|^2 df \approx \tfrac{1}{2}\nu\langle B_n^2\rangle\int_{-\infty}^{+\infty}|S(f)|^2 df. \quad (9)$$

The fractional rms intensity variation caused by the red noise is $\gamma_{\rm RN} = (P_{\rm RN}/P_0)^{1/2}$ whereas that caused by the oscillation at f_n is $\gamma_n = (P_n/P_0)^{1/2}$.

At some points in the following sections we shall also make use of a *simplified reference spectrum*, namely, the particular example of the reference spectrum (6) that is produced by a purely sinusoidal modulation function. For such a modulation function, all the coefficients B_n vanish except for one. We denote the frequency of the resulting single peak in the power spectrum f_p and the power density $\langle P(f)\rangle_{\rm ref\ 1}$.

III. EFFECT OF PULSE SHAPE

The *total* power in the red noise and in the oscillations depends on the shape of the pulse envelope whereas the *ratio* of the power in the oscillations to that in the red noise is sensitive to the mean value of the pulse and its harmonic content. In this section we illustrate this behavior with random processes in which the pulse time and initial phase are uniformly distributed and uncorrelated and the other parameters describing the pulse shape are independent of time. With these simplifying assumptions the power-density spectrum is the reference spectrum of equation (6).

a) *Dependence of Spectrum on Envelope Function*

In order to illustrate the effect of the shape of the pulse envelope on the power spectrum, we compare in Table 1 the spectral function $|S(f)|^2$ and the total power in the red noise

TABLE 1

EFFECT OF ENVELOPE FUNCTION ON POWER SPECTRUM

Power Density or Total Power[a]	Exponential Envelope[b]	Rectangular Envelope[c]
$\lvert S(f)\rvert^2$	$\dfrac{\tau^2}{1+(2\pi f\tau)^2}$	$\tau^2\left(\dfrac{\sin \pi f\tau}{\pi f\tau}\right)^2$
$P_{\rm RN}$	$\frac{1}{2}\langle A^2\rangle\langle N\rangle$	$\langle A^2\rangle\langle N\rangle$
P_n	$\frac{1}{4}\langle B_n^2\rangle\langle N\rangle$	$\frac{1}{2}\langle B_n^2\rangle\langle N\rangle$

[a] $P_{\rm RN}$ and P_n denote the total power in the red-noise component and nth harmonic peak, respectively.

[b] $G(t) = \theta(t)\exp(-t/\tau)$; $\langle N\rangle \equiv \nu\tau$ is the mean number of pulses occurring in time τ.

[c] $G(t) = 1$, $0 \le t \le \tau$; 0, $|t| > \tau$; $\langle N\rangle \equiv \nu\tau$ is the mean number of pulses occurring in time τ.

and nth harmonic for reference spectra produced by pulses with exponential envelopes of decay time τ and pulses with rectangular envelopes of duration τ. Both envelope functions have been normalized according to equation (4). Note that for a given modulation function, *the ratio of the total power in the red noise to that in the oscillations does not depend on the shape of the envelope function.* However, the *total power* in these spectral components, and hence their power density relative to the Poissonian noise, does depend weakly on the shape of $G(t)$.

b) Dependence of Spectrum on Modulation Function

The ratio of the power in the oscillations to that in the red noise depends on both the mean value and the harmonic content of the modulation function. For example, if the mean value of every disturbance of the X-ray intensity is zero ($A_i = 0$ in eq. [5] for all i), then $\langle A^2 \rangle = 0$ and there is no red noise at all (see Table 1). However, if any of the pulses have nonzero mean, red noise is unavoidable. In the case of a purely sinusoidal modulation function ($B_n \neq 0$ for only one value of n, say m), the requirement that each pulse be positive at all times ($H \geq 0$) implies $A_i \geq B_{mi}$ and hence $P_{\rm RN} \geq 2P_m$. Although the red noise may be suppressed to some extent by interactions between fluctuations and the magnetosphere that reduce $\langle A_i \rangle$ (see § II), to suppress the red noise by a large factor in this way requires finely tuned interaction and hence appears unlikely.

On the other hand, even for pulses that are positive at all times, the total power in the oscillations may be larger than that in the red noise if the modulation function is sharply peaked. To illustrate this effect, consider the modulation function

$$\mathrm{H}(t) = A_q \cos^{2q} [(2\pi f_B t + \phi)/2] \, . \qquad (10)$$

Here the parameter q is a measure of the degree to which the oscillations are peaked in time: larger values of q correspond to oscillations that are sharper. The total power in the peaks at the beat frequency and its overtones, relative to the total power in the red noise, is listed in Table 2 for values of q ranging from 1 to 5. The more sharply peaked are the oscillations, the greater is the power in the oscillations relative to that in the red noise. For $q \geq 3$, the power in the fundamental exceeds that in the red noise. This increase in the strength of the fundamental relative to the red noise is, of course, accompanied by the appearance of power at overtones of the beat frequency.

The effect on the power density spectrum is illustrated in Figure 3, which shows the spectra corresponding to $q = 1$ and $q = 3$, assuming an exponential envelope function.[6] The increase in the power in the oscillations relative to that in the red noise as q changes from 1 to 3 may be clearly seen, as well as the appearance of a peak at the first overtone (the power in the second overtone is too small to be seen clearly in this figure). The spectrum of Figure 3*b* agrees qualitatively with the spectrum of GX 5 − 1 reported by van der Klis *et al.* (1985*b*) at 2277–2486 counts per second.

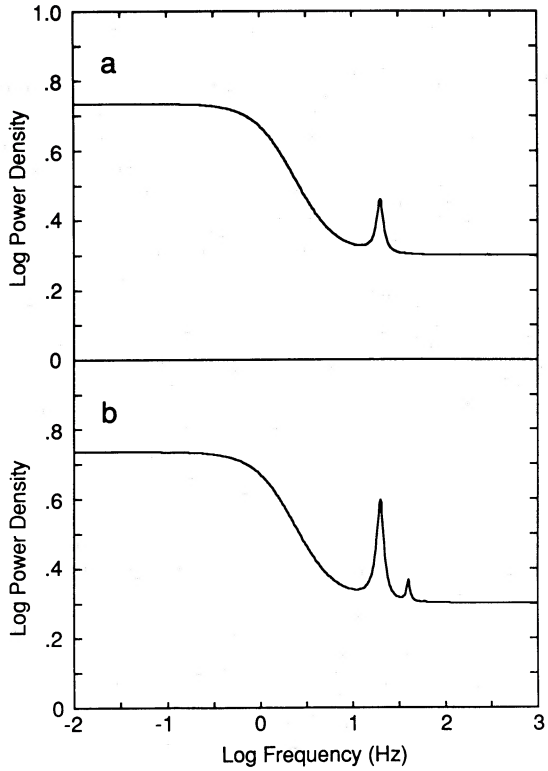

FIG. 3.—Sample power spectra illustrating the effect of the sharpness in time of the oscillations in the pulse wave form on the power spectrum. (*a*) Spectrum for the modulation function of eq. (10) with $q = 1$. (*b*) Spectrum for the modulation function of equation (10) with $q = 3$. The Poissonian noise, the red noise, and the oscillation peaks at one or more harmonics of f_B may be clearly seen. Both spectra assume an exponential envelope function, $f_B = 20$ Hz, $\tau = 0.0853$ s, and $2\langle A^2 \rangle^{1/2}/\tau = 469$. The $q = 3$ spectrum agrees qualitatively with the 0.1–1000 Hz spectrum of GX 5 − 1 reported in Fig. 4*a* of van der Klis *et al.* (1985*b*). Note the increase in the power at the fundamental as well as the appearance of power at the first overtone as q increases (for $q = 3$, the peak at the second overtone is too small to be seen clearly here).

[6] Here and in all the other spectra displayed below, the power density has been normalized by dividing by the mean intensity $\langle I \rangle$ in order to facilitate comparison with observational results (see Leahy *et al.* 1983). For the same reason, $\langle A_q \rangle$ has been adjusted to keep $\langle I \rangle$ the same for all spectra.

TABLE 2

EFFECT OF MODULATION FUNCTION ON POWER SPECTRUM[a]

q	$P_{\rm RN}$	P_1	P_2	P_3	P_4	P_5
1.....	1	0.50	...	...	...	...
2.....	1	0.89	0.056	...	...	...
3.....	1	1.13	0.18	0.005	...	...
4.....	1	1.28	0.32	0.026	4×10^{-4}	...
5.....	1	1.39	0.45	0.064	0.003	3×10^{-5}

[a] For the modulation function $H(t) = A_q \cos^{2q} [(2\pi f_B t + \phi)/2]$. Here P_1, P_2, and P_3 are the total power in the peaks at $f_1 = f_B, f_2 = 2f_B, \ldots, f_5 = 5f_B$. All powers have been normalized to the total power $P_{\rm RN}$ in the red-noise component of the spectrum.

IV. EFFECTS OF FREQUENCY AND LIFETIME DISTRIBUTIONS

Up to now, we have assumed that the orbital frequencies and lifetimes of all fluctuations in the boundary layer are the same. If this were true, the beat frequency f_B and the pulse duration τ would be the same for all pulses. However, both physical arguments and the observed spectra suggest there should be a spread in the values of both quantities. In this section we illustrate the effect of such spreads on the power spectrum with several relatively simple models. Analytical expressions suitable for fitting to observed spectra are given in the Appendix.

There are two physical phenomena that may be expected to require the introduction of a distribution of beat frequencies. First, fluctuations may form at different radii within the

boundary layer. At different radii, the fluctuations have different orbital velocities, due to the variation of the Keplerian orbital velocity with radius, and hence their beat frequencies are different. To the extent that the radius and hence the beat frequency of each fluctuation is constant, this phenomenon may be described accurately by introducing a distribution of beat frequencies that reflects the radial distribution of fluctuations.

Second, fluctuations entering the boundary layer or forming there may be expected to drift radially inward. In this case, the radius and hence the beat frequency of each fluctuation changes slightly with time. If the change in frequency is small compared to $1/\tau$, this phenomenon may be described accurately by introducing a distribution of beat frequencies that reflects the time that each fluctuation spends at a given radius. However, if the change in frequency is not small, this phenomenon causes wiggles to appear in the wings of the oscillation peaks (Alpar 1986). This phenomenon is discussed in more detail in § VIII.

Both phenomena arise from the azimuthal velocity shear in the boundary layer and contribute to the breadth of the oscillation peaks in the power spectrum. We therefore refer to both phenomena as shear broadening. The finite lifetime of the fluctuations and hence of the X-ray pulses they produce also contributes to the width of the oscillation peaks. The lifetime of the fluctuations also has a major effect on the shape of the red-noise component of the power spectrum. On physical grounds we expect a distribution of fluctuation lifetimes rather than a single lifetime for all fluctuations.

The effect on the power spectrum of spreads in the beat frequencies and lifetimes of the density fluctuations is obtained by averaging equation (6) over the appropriate joint distribution function $\rho([f_B - \langle f_B\rangle]/\Delta f_B, \tau)$. In the red-noise term, the result is that $|S(f)|^2$ is replaced by the averaged function $\langle|S(f)|^2\rangle$, where only the average over the τ-distribution is relevant, since $S(f)$ is independent of f_B. In the oscillation terms, the averaging process is equivalent to convolving $|S(f - nf_B)|^2$ with $\rho([f_B - \langle f_B\rangle]/\Delta f_B, \tau)$. Thus, if both $|S(f - nf_B)|^2$ and the beat-frequency distribution may be approximated by Lorentzians (or Gaussians), the averaged peak shape is a Lorentzian (or Gaussian). The result is that the averaged power density spectrum $\langle P(f)\rangle_{\rm ave}$ has peaks at $f_n = n\langle f_B\rangle$, where $\langle f_B\rangle$ is the average beat frequency, with HWHMs that are, loosely speaking, the sum of the width Δf_L produced by the finite duration of the pulse and the width $n\Delta f_B$ caused by the spread Δf_B in beat frequencies. Note that *lifetime broadening affects all the peaks equally whereas the effect of shear broadening increases linearly with harmonic number n.*

The characteristics of the power spectra reported so far for GX 5−1 and Cyg X-2 may be reproduced by relatively simple distributions. For simplicity we therefore assume that f_B and τ are uncorrelated so that $\rho(f_B, \tau)$ may be written $\rho(f_B)\rho(\tau)$. Fits of reference spectra to the spectra reported in GX 5−1 (see Paper I) indicate that the width of the f_B-distribution is narrow compared to f_B itself. Thus, the f_B-distribution should be represented by a function that is fairly sharply peaked. In order to eliminate the envelope function as a source of variation from one spectrum to another we shall adopt the same envelope function for all the power spectra that we plot as well as for the analytic calculations described in the Appendix. Since an exponential envelope function appears adequate to describe most of the data available at present we adopt it. Having made this choice, the averaging calculations are greatly simplified if we choose a Lorentzian beat-frequency distribution, since then the convolution property noted above may be used. We therefore assume that $\rho(f_B)$ can be adequately represented by the distribution

$$\rho(f_B) = \frac{\Delta f_B}{\pi}\,\frac{1}{(\Delta f_B)^2 + (f_B - \langle f_B\rangle)^2}\,. \tag{11}$$

Here Δf_B is the HWHM of the f_B-distribution.

According to van der Klis *et al.* (1985*a*, *b*), in GX 5−1 the power density increases smoothly with decreasing frequency down to the lowest frequencies ($\sim$0.03 Hz) that have been observed. In order to reproduce such a spectrum with the random-process model of § II, the distribution in pulse duration must be relatively broad. We therefore model the τ-distribution as a power law, namely,

$$\begin{aligned} \rho(\tau) &= 0\,, && \tau < \tau_1 \\ &= K\tau^{-m}\,, && \tau_1 \le \tau \le \tau_2\,, \\ &= 0\,, && \tau > \tau_2 \end{aligned} \tag{12}$$

where the constant K is chosen to normalize the distribution to unit area.

The Appendix summarizes the steps involved in averaging equation (6) over the distributions (11) and (12) and provides analytical expressions suitable for fitting to observed spectra. The effects on the power spectrum of these frequency and lifetime distributions are illustrated in Figures 4–6.

Figure 4 shows how the power spectrum is affected by changes in the power-law index m of the lifetime distribution with τ_1 and τ_2 fixed. Larger positive values of m correspond to lifetime distributions that fall more steeply with increasing lifetime and hence shorter mean lives. Shorter mean lives produce broader oscillation peaks, slower increases in the power density of the red-noise component at low frequency, and—since the spectral function $|S(f)|^2$ is $\propto\tau^2$ at low frequency—less power density in the red noise there. For the same reason, the total power in the oscillations, and hence the power density in the peaks relative to the power density in the Poissonian noise, decreases rapidly with decreasing mean τ. The spectrum shown in Figure 4*c* agrees qualitatively with that reported by van der Klis *et al.* (1985*b*) for GX 5−1 at 2277–2486 counts per second.

Figure 5 illustrates how the spectrum is affected by changes in the width of the lifetime distribution, if the power-law index of the distribution is fixed and moderately large ($m = 3$). Except for Figure 5*c*, these spectra show what happens when τ_1 is progressively decreased while τ_2 is held fixed. For $m = 3$, the mean life decreases with decreasing τ_1 for fixed τ_2, again causing the oscillation peaks to broaden, the red-noise spectrum to flatten, and the oscillations to weaken. Comparison of Figures 5*b* and 5*c* shows clearly that the shape of the red-noise spectrum at low frequencies is sensitive to the lifetimes of the longest lived pulses, even if the lifetime distribution is steeply decreasing: the red-noise power density rises with decreasing frequency down to $f \approx 1/2\pi\tau_2$ and then flattens at still lower frequencies. The spectrum of Figure 5*b* agrees qualitatively with the spectrum of GX 5−1 mentioned above.

Finally, Figure 6 illustrates the effect of a spread in beat frequencies on the power spectrum. For the (Lorentzian) distribution assumed here, changes in the width of the beat-frequency distribution affect equally the relative widths $\Delta f_n/f_n$ of the fundamental and the overtones. The beat-frequency dis-

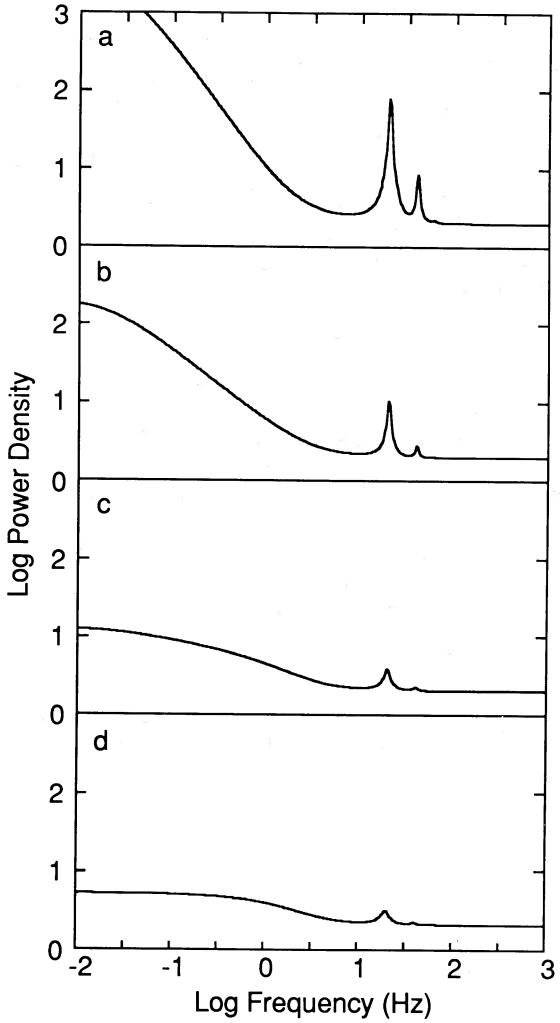

FIG. 4.—Sample power spectra illustrating the effect of the power-law index of the fluctuation lifetime distribution on the spectrum of the red noise and the height of the oscillation peaks. (*a*) $m = 1$. (*b*) $m = 2$. (*c*) $m = 3$. (*d*) $m = 4$. All four spectra assume an exponential envelope function, the modulation function of equation (10) with $q = 3$, the Lorentzian beat-frequency distribution (11) with $\langle f_B \rangle = 20$ Hz and $\Delta f_B = 0.8$ Hz, the power-law lifetime distribution (12) with $\tau_1 = 0.05$ s and $\tau_2 = 10$ s, and $2\nu\langle A^2 \rangle / \langle I \rangle = 400$.

tribution has no effect on the red-noise component of the spectrum.

V. EFFECT OF NONUNIFORM PHASE DISTRIBUTIONS

The variation of the magnetospheric field and plasma density with azimuth around the boundary layer (see § II*a*) may cause fluctuations to drift from the inner disk into the boundary layer preferentially at certain azimuths. Such a situation may be described in the framework of the random process model of § II by a nonuniform distribution $\rho(\phi_i)$ of the phases ϕ_i of the X-ray intensity disturbances caused by the fluctuations, at the times t_i that they are produced. If $\rho(\phi_i)$ is nonuniform, the oscillation and red-noise amplitudes interfere, distorting the shape of the power-density spectrum with respect to the reference spectrum. In the present section we examine this effect.

In order to show clearly the effect of the distribution of pulse phases on the spectrum, we consider the simple case of a purely sinusoidal modulation function, namely,

$$H(t) = A + B \cos(2\pi f_p t + n\phi), \tag{13}$$

where f_p is the nth harmonic of the beat frequency f_B. We assume that the density fluctuations occur at random times (i.e., that t_i is uniformly distributed in time), that ϕ_i and t_i are uncorrelated, and that the distributions of the initial phases ϕ_i are the same for all pulses. Then the power spectrum of the time series (2) with the envelope function (4) is

$$\begin{aligned}\langle P(f) \rangle = \langle P(f) \rangle_{\text{ref 1}} &+ 2\nu\langle AB \rangle \,\text{Real}\left\{[S(f)S^*(f-f_p) + S^*(f)S(f+f_p)] \times \int_0^{2\pi} \rho(\phi) e^{-in\phi} d\phi \right\} \\ &+ \nu\langle B^2 \rangle \,\text{Real}\left[S(f-f_p)S^*(f+f_p) \int_0^{2\pi} e^{i2n\phi} \rho(\phi) d\phi \right].\end{aligned} \tag{14}$$

Here $\langle P(f) \rangle_{\text{ref 1}}$ is the simplified reference spectrum defined at

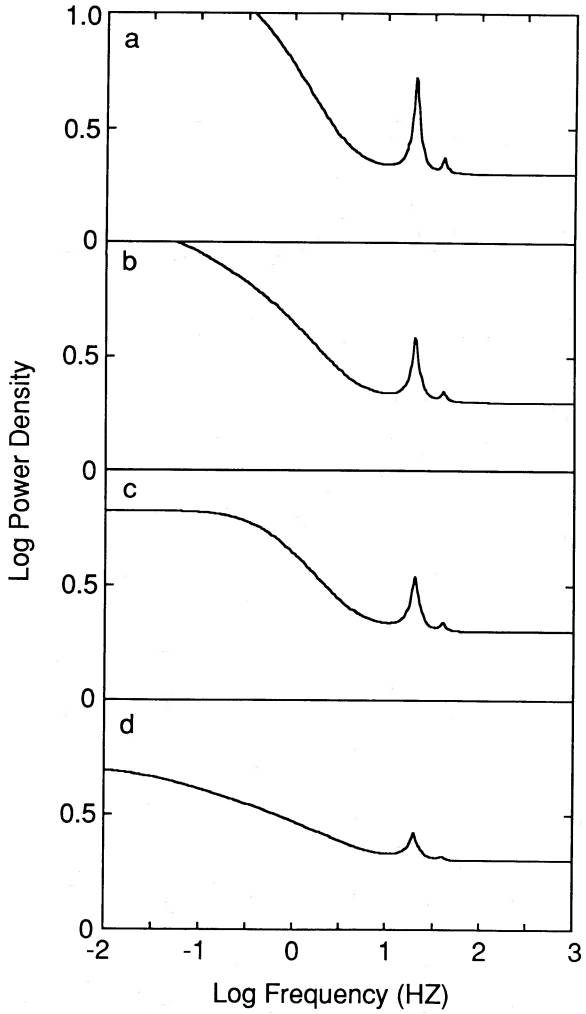

FIG. 5.—Sample power spectra illustrating the effect of the width of the fluctuation lifetime distribution on the spectrum of the red noise and the height of the oscillation peaks. (*a*) $\tau_1 = 0.075$ s, $\tau_2 = 10$ s. (*b*) $\tau_1 = 0.05$ s, $\tau_2 = 10$ s. (*c*) $\tau_1 = 0.05$ s, $\tau_2 = 0.5$ s. (*d*) $\tau_1 = 0.025$ s, $\tau_2 = 10$ s. All four spectra assume an exponental envelope function, the modulation function of eq. (10) with $q = 3$, the Lorentzian beat-frequency distribution (11) with $\langle f_B \rangle = 20$ Hz and $\Delta f_B = 0.8$ Hz, the power-law lifetime distribution (12) with $m = 3$, and $2\nu\langle A^2 \rangle / \langle I \rangle = 400$.

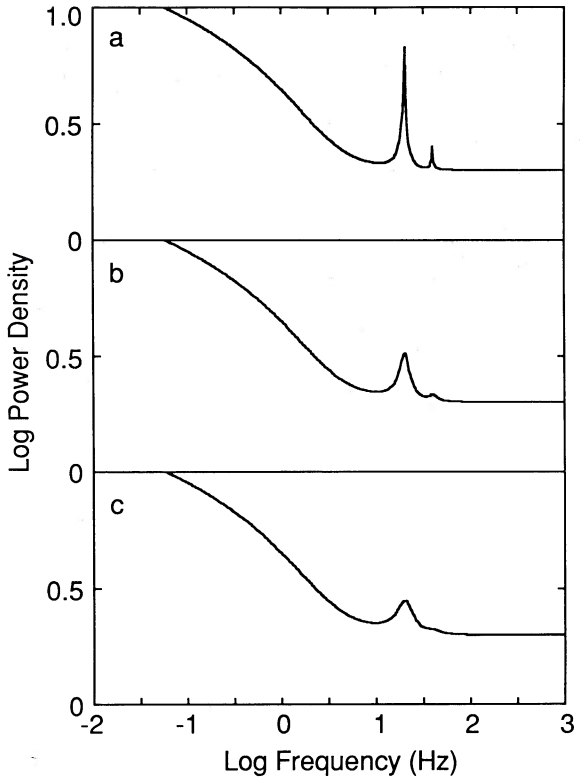

FIG. 6.—Sample power spectra illustrating the effect of the beat-frequency distribution on the shape of the oscillation peaks. (*a*) $\Delta f_B = 0$ Hz. (*b*) $\Delta f_B = 1.6$ Hz. (*c*) $\Delta f_B = 3.2$ Hz. All three spectra assume an exponential envelope function, the modulation function of eq. (10) with $q = 3$, the Lorentzian beat-frequency distribution (11) with $\langle f_B \rangle = 20$ Hz, the power-law lifetime distribution (12) with $\tau_1 = 0.05$ s, $\tau_2 = 10$ s, and $m = 3$, and $2\nu\langle A^2\rangle/\langle I\rangle = 400$.

the end of § II, $S^*(f)$ is the complex conjugate of $S(f)$, and $\rho(\phi)$ is the distribution of initial phases, normalized according to

$$\int_0^{2\pi} \rho(\phi) d\phi = 1 \,. \tag{15}$$

If the initial phases ϕ are uniformly distributed, $\rho(\phi) = 1/2\pi$ and the last two terms in equation (14) vanish. However, if the ϕ_i are not uniformly distributed, these two terms usually do not vanish. Thus, they describe the effect of nonuniformity in the initial phase distribution.

We can make a quantitative estimate of the distortion of the spectrum caused by a nonuniform distribution of initial phases in the special case of fluctuations which are all regions of above-average plasma density. In this case the disturbance of the X-ray intensity caused by each fluctuation is positive at all times, A must equal or exceed B in equation (13) for every pulse, the second term on the right side of equation (14) is comparable to or greater than the third term, and we can estimate the distortion by comparing this term with the red noise and QPO term in the simple reference spectrum. The largest distortion occurs at $f \approx f_p$, where the second term is $\approx (B/A)|S(f_p)/S(0)|$ compared to the red-noise term in the simple reference spectrum and $\sim 4(A/B)|S(f_p)/S(0)|$ compared to the QPO term. Since $|S(f_p)| \leq |S(0)|$, the distortion of the red-noise spectrum is always less than unity. Similarly, if the fluctuation lifetime is long ($\tau \gg 1/2\pi f_p$) and $A \approx B$, then $|S(f_p)| \ll |S(0)|$ and the distortion of the QPO peak is small; however, if $\tau \lesssim 1/2\pi f_B$, the distortion will be of order unity or greater. If $\tau \gg 1/2\pi f_B$ but $A \gg B$, the distortion may be substantial, depending on the values of $2\pi f_B \tau$ and A/B, but the total power in the QPO is small compared to that in the red noise.

In order to get more of a feeling for the size and character of the distortions produced by nonuniform initial phase distributions, consider the extreme situation in which all fluctuations form within the boundary layer or enter it at the same stellar azimuth ϕ_0. The initial phase distribution that describes this situation is

$$\rho(\phi) = \delta(\phi - \phi_0) \,. \tag{16}$$

Figure 7 shows the resulting spectra, for $A = B$ and $\phi_0 = 0°$, 90°, 180°, and 270°.

The shape of the spectrum near the valley in the power density created by the fall of the red-noise power density and the rise of the QPO power density with increasing frequency appears to be the most sensitive diagnostic of the distribution of initial pulse phases. This valley becomes considerably deeper (shallower) than in the reference spectrum for $\phi_0 = 0°$ (180°), due to destructive (constructive) interference between the red noise and QPO amplitudes. This effect is particularly strong when τ is small, since in this case the red noise and QPO components of the spectrum tend to overlap.

For $\phi_0 = 0°$ (180°) the shape of the QPO peak is also affected by the distribution of initial pulse phases, becoming asymmetric due to the decrease (increase) in the power density at frequencies just below f_B and a corresponding increase (decrease) in the power density just above; as a result, the

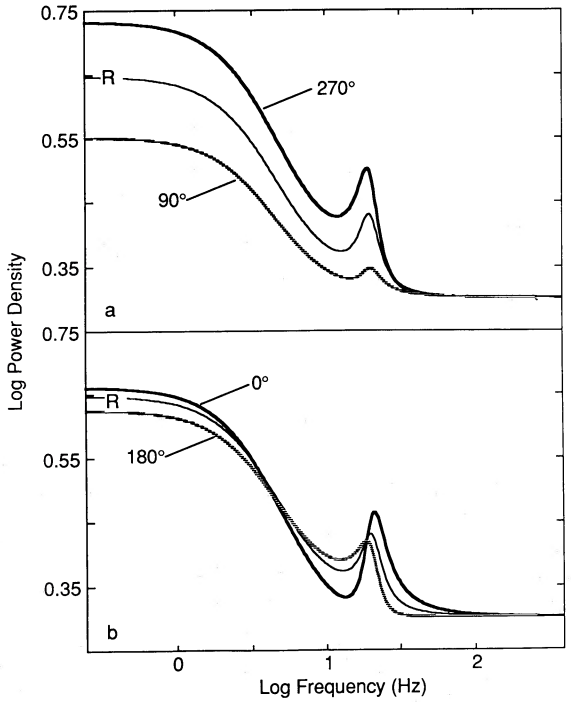

FIG. 7.—Sample power spectra showing the effect of nonuniform distributions of the initial stellar azimuths ϕ_0 of fluctuations in the boundary layer. (*a*) Comparison of spectra with $\phi_0 = 90°$ and 270° with the reference spectrum *R*. (*b*) Comparison of spectra with $\phi_0 = 0°$ and 180° with the reference spectrum *R*. All spectra assume an exponential envelope function, the modulation function of eq. (13) with $f_p = 20$ Hz, $\tau = 0.04$ s, $\langle B^2\rangle/\langle A^2\rangle = 1$, and $2\langle A^2\rangle^{1/2}/\tau = 1500$.

centroid frequency of the QPO peak is displaced slightly to higher (lower) frequency. On the other hand, for $\phi_0 = 90°$ or 270° the shape of the peak at f_p remains almost the same as in the reference spectrum, although the overall power density in the red noise and QPO components is slightly decreased (increased).

VI. EFFECT OF NONUNIFORM TIME DISTRIBUTIONS

A nonuniform distribution of pulse times, produced by variations in the rate at which fluctuations enter the boundary layer, can produce features in the power-density spectrum even if the time-averaged mass accretion rate, and hence the mean X-ray intensity, remains constant. The effect of nonuniform pulse rates may be studied by considering nonuniform distributions of the pulse time t_i. In order to illustrate the effect that such nonuniform distributions can have on the power spectrum, we consider the simple case in which there is no correlation between the initial phase ϕ_i and the time t_i of the ith pulse, the distributions of initial phases and times are the same for all pulses, the initial phases are uniformly distributed, and the modulation function is purely sinusoidal, as in equation (13).

Averaging the Fourier transform of the intensity time series produced by exactly N density fluctuations over the uniform phase distribution gives

$$|S_N(f)|^2 = A^2|S(f)|^2(N + R) + \frac{B^2}{4} \times N[|S(f-f_p)|^2 + |S(f+f_p)|^2] , \quad (17)$$

where A and B have been assumed, for simplicity, to have the same values for all pulses. The term that describes the effect of a possibly nonuniform t_i-distribution is

$$R = \sum_{j\neq k}^{N}\sum^{N} e^{-i2\pi f(t_j - t_k)} . \quad (18)$$

If the t_i-distribution is uniform, R vanishes after equation (17) is averaged with respect to t_i.

Equation (17) shows that the t_i-distribution does not affect the oscillation peak but only the red-noise spectrum. Averaging R over an arbitrary t_i-distribution $p_T(t)$ yields

$$\bar{R} = \int_0^T p_T(t_1)dt_1 \ldots \int_0^T p_T(t_N)dt_N \sum_{j\neq k}^{N}\sum^{N} e^{-i2\pi f(t_j - t_k)} = N(N-1)\left|\int_0^T p_T(t)e^{-i2\pi f t}dt\right|^2 \geq 0 , \quad (19)$$

where $p_T(t)$ is normalized according to

$$\int_0^T p_T(t)dt = 1 \quad (20)$$

and the measurement time interval T has been assumed much longer than τ. The result (19) shows that *any nonuniformity in the t_i-distribution can only increase the strength of the red noise.*

Consider now two specific examples of nonuniform t_i-distributions that illustrate the effects of clustering of fluctuations in time. First, suppose that a cluster of n fluctuations arises within the boundary layer or enters it at time t_{cj}. Assume that the initial stellar azimuths of the fluctuations are uniformly distributed and that the times t_{cj} at which the clusters enter the boundary layer are uniformly distributed in time. Then the power spectrum is

$$\langle P(f)\rangle = \langle\overline{P(f)}\rangle_{\text{ref 1}} + 2\bar{\nu}\langle A\rangle^2\left(\frac{\langle n^2\rangle}{\langle n\rangle} - 1\right)|S(f)|^2 , \quad (21)$$

where $\bar{\nu}$ is the time-averaged rate at which fluctuations enter the boundary layer over time T. $\langle\overline{P(f)}\rangle_{\text{ref 1}}$ is given by $\langle P(f)\rangle_{\text{ref 1}}$ with $\langle I\rangle$ and ν replaced by $\langle\bar{I}\rangle$ and $\langle\bar{\nu}\rangle$. The result (21) shows that the shape of the red noise spectrum is unaffected, but its strength is increased by the factor $(\langle n^2\rangle/\langle n\rangle - 1)(\langle A\rangle^2/\langle A^2\rangle)$.

Second, suppose the probability of a fluctuation entering the boundary layer varies periodically in time according to the distribution

$$p_T(t) = \frac{a}{T}(1 + b\cos 2\pi f_0 t) , \quad (22)$$

where a is a constant chosen so that $p_T(t)$ satisfies equation (20). The resulting power spectrum is

$$\langle P(f)\rangle = \langle\overline{P(f)}\rangle_{\text{ref 1}} + 2\bar{\nu}\langle A\rangle^2|S(f_0)|^2\tfrac{1}{4}\bar{\nu}\langle b\rangle^2\delta(f - f_0) . \quad (23)$$

In a more realistic model the peak at f_0 produced by the oscillations in the pulse rate would be broadened. Note that the peak at f_0 can in principle be distinguished from the peak at f_p produced by the oscillations in the pulse wave forms by the fact that its width is independent of the shape of the red-noise spectrum. Since the strength of the feature at f_0 is proportional to $|S(f_0)|^2$, such a feature will be most apparent if it is on the shoulder of the red noise, where $|S(f)|^2$ is relatively large. An example of such a spectrum is shown in Figure 8.

VII. EFFECTS OF CORRELATIONS BETWEEN PHASE AND TIME

As mentioned in § II, several mechanisms may cause fluctuations in the boundary layer to be spatially clustered. For example, interaction of the magnetosphere with persistent density patterns in the inner disk (see Zurek and Benz 1986) may cause the density of plasma in the boundary layer to vary in phase with the density variation in the inner disk, producing

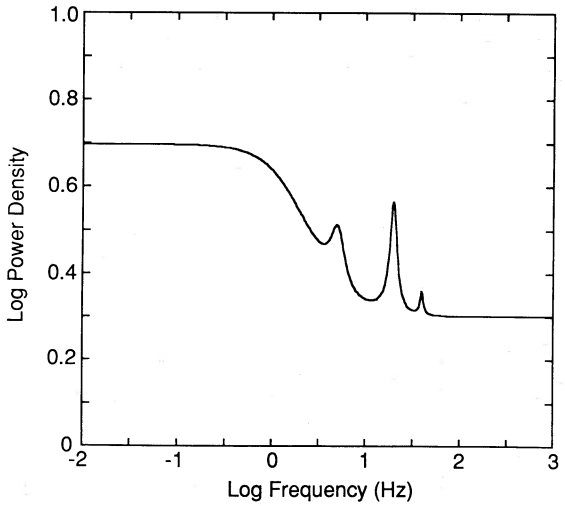

FIG. 8.—Sample power spectrum showing how periodic variation of the pulse rate produces a peak in the spectrum in addition to the QPO peaks. This example assumes an exponential envelope function, the modulation function of eq. (10) with $q = 3$ and $f_B = 20$ Hz, $\tau = 0.0853$ s, $2\bar{\nu}\langle A^2\rangle/\langle\bar{I}\rangle = 400$, $f_0 = 5$ Hz, $\Delta f_0 = 1$ Hz, $\langle b\rangle^2\bar{\nu} = 30$, and $\langle A^2\rangle = \langle A\rangle^2$.

spatial clustering of fluctuations in the boundary layer. Interaction of the magnetosphere with larger fluctuations in the inner disk may cause them to fragment into smaller but more numerous fluctuations. If these drift into the boundary layer at random times but at the azimuth of the larger fluctuation from which they came, there will be a local excess of fluctuations at the position where the original larger fluctuation would have been. Similarly, if the existence of a slight local excess of plasma orbiting in the boundary layer causes, by loading nearby magnetospheric-field lines with plasma or some other mechanism, an enhancement in the rate of plasma entry from the inner disk into the boundary layer at the instantaneous azimuth of the excess, the excess density may persist. The resulting spatial clusters of fluctuations create pulse-to-pulse correlations in the phases of the oscillating components of the X-ray pulses they produce. Even a small correlation of this type can have a dramatic effect on the power spectrum, greatly increasing the power in the oscillation peaks relative to that in the red noise.

As a simple example of this effect, consider a model in which the phases of the jth and kth pulses with origins in time at t_j and t_k satisfy

$$\phi_j - \phi_k = 2\pi f_B(t_j - t_k)\,, \tag{24}$$

with t_j and t_k uniformly distributed in time. The phase correlation (24) between X-ray pulses corresponds physically to a local enhancement in the density of fluctuations in the boundary layer at a position comoving with the plasma orbiting there, as in Figure 2, caused by fluctuations entering the boundary layer at the instantaneous azimuth of the cluster. The assumption that t_j and t_k are uniformly distributed in time means that the fluctuations enter the boundary layer at random times; equation (24) then implies that although they enter at fixed azimuths *in the frame corotating with the boundary layer plasma*, they enter at random azimuths *in the frame of the star*.[7]

As an illustration of the behavior that results from spatial clustering, let us assume as before an exponential envelope function and the modulation function of equation (5). In order to understand the nature of the X-ray intensity time series, it may be helpful to consider first the autocorrelation function of the intensity since in the physical model described in § II this function simply reflects the time development of the plasma density-density correlation function in the boundary layer at the azimuth(s) at which the accretion rate to the stellar surface is relatively large. The intensity autocorrelation function is

$$\langle \Psi(\Delta t)\rangle = \langle I\rangle\delta(\Delta t) + \langle I\rangle^2 + \tfrac{1}{2}\langle N\rangle \times \left[\langle A^2\rangle + \tfrac{1}{2}\sum_{n=1}^{\infty}\langle B_n^2\rangle \cos(2\pi n f_B \Delta t)\right] \times e^{-|\Delta t|/\tau} + \tfrac{1}{2}\eta\langle N\rangle^2 \sum_{n=1}^{\infty}\langle B_n\rangle^2 \cos(2\pi n f_B \Delta t)\,. \tag{25}$$

The terms in this function may be understood as follows. The first term represents the autocorrelation of the Poissonian noise. The second describes the mean intensity, which is independent of the lag Δt. The third term, which is proportional to $\langle N\rangle$, represents the correlation of the wave forms produced by the individual fluctuations with themselves. This "incoherent" term decays exponentially in a time τ due to the disappearance of the individual fluctuations on this time scale. The fourth term, which is proportional to $\eta\langle N\rangle^2$, describes the fact that oscillations persist with the same phase as long as the cluster persists. This "coherent" term is present because new fluctuations that enter an existing cluster contribute an oscillating X-ray intensity with the same phase as the existing oscillations. Since by assumption these new fluctuations enter at random times, there is no corresponding "coherent" term produced by the mean intensity of the individual pulses. The correlation coefficient η expresses the degree of clustering of the fluctuations (see below).

An example of the behavior of the normalized correlation function $\langle \Psi'(\Delta t)\rangle \equiv [\langle \Psi(\Delta t)\rangle - \langle I\rangle\delta t - \langle I\rangle^2]/[\langle N\rangle\langle A^2\rangle/2]$ is shown in Figure 9. The correlation is of course a maximum at $\Delta t = 0$. It falls slightly for lags $\Delta t \approx \tau$, as the autocorrelation of the pulses produced by the individual fluctuations is lost, due to their gradual disappearance; however, a high degree of correlation persists in the oscillations, because the oscillating components of the pulses produced by the new fluctuations are in phase with those produced by the fluctuations that have disappeared. This correlation persists as long as the local enhancement in the density of fluctuations persists.

The power spectrum corresponding to the autocorrelation function of equation (25) is

$$\langle P(f)\rangle = \langle P(f)\rangle_{\rm ref} + \tfrac{1}{2}\eta\langle N\rangle^2 \sum_{n=1}^{\infty}\langle B_n\rangle^2 \delta(f - nf_B)\,, \tag{26}$$

where the first term on the right is the "incoherent" reference spectrum of equation (6). The second term, which we refer to as the coherent QPO spectrum, represents the additional power at the harmonics $f = nf_B$ produced by spatial clustering of fluctuations in the boundary layer.

The spectrum (26) illustrates two important effects of clustering. First, it increases the strength of the quasi-periodic oscillations relative to the red noise in the spectrum. This is because the power in the coherent spectrum is proportional to $\langle N\rangle^2$, whereas the power in the incoherent spectrum, which includes the incoherent oscillations and the red noise, is pro-

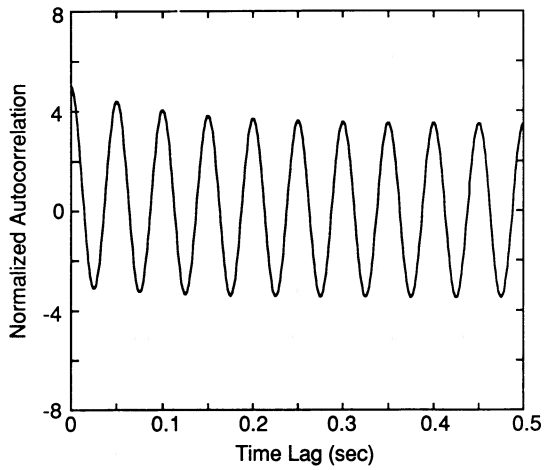

FIG. 9.—Autocorrelation function for the simplified model discussed in the text, showing the effects of pulse-to-pulse correlations in the phases of the oscillating components in the pulse wave forms. This example assumes an exponential envelope function, the modulation function of equation (10) with $q = 1$ and $f_B = 20$ Hz, $\tau = 0.1$ s, $\langle A^2\rangle = \langle A\rangle^2$, and $2\langle A^2\rangle^{1/2}/\tau = 469$. The correlation strength parameter $\eta\nu$ is 35.

[7] The times t_j and t_k can be uniformly distributed only while the cluster persists. On time scales longer than the lifetime of the cluster its appearance and disappearance, and the resulting nonuniform distribution of pulse times, will be apparent, causing an increase in the red-noise power density at frequencies comparable to the inverse of the cluster lifetime.

portional to $\langle N \rangle$. The ratio of the power in the QPO peak to the power in the red noise is $(1/2)(\langle B^2 \rangle / \langle A^2 \rangle) + \eta \langle N \rangle (\langle B \rangle^2 / \langle A^2 \rangle)$. Thus, if there are as expected many fluctuations in the boundary layer (see Paper I), the power in the QPO peak may be much greater than the power in the red noise, even for a small amount of clustering. For example, if there are m clusters in the boundary layer each with an angular extent less than 90° (see Fig. 2) and containing *altogether* a fraction ξ of *all* the density fluctuations, then $\eta = \xi^2/m$.

Second, the widths of the coherent QPO peaks do not depend on the lifetimes of the individual fluctuations but only on the lifetimes of the clusters (assumed infinite in the simple model of eq. [25]). Thus, the lifetimes τ of the individual fluctuations and the spread Δf_c in the orbital frequencies of the fluctuations affect different components of the spectrum: τ determines the location of the shoulder in the red-noise spectrum, whereas Δf_c determines the spread Δf_B in beat frequencies and hence the widths of the QPO peaks. This contrasts with the incoherent spectra discussed previously, in which both τ and Δf_B contribute to the widths of the QPO peaks. The lifetime distribution *does* affect the *strength* of the coherent component of the spectrum through the relation $\langle N \rangle = \nu \langle \tau \rangle$. Although the widths of the peaks in the coherent spectrum are less than those in the incoherent spectrum, the relative strengths of the various harmonics of the beat frequency are the same in the two spectra.

In reality, shear broadening will cause the QPO peaks to have finite widths, even if the clusters were to persist indefinitely. For example, if the beat frequencies of the fluctuations are distributed according to equation (11) and the *individual* fluctuations have lifetimes distributed according to equation (12), the power spectrum of the intensity time series is

$$\langle P(f) \rangle = \langle P(f) \rangle_{\rm ave} + \frac{1}{2} \eta \nu^2 g(m, \tau_1, \tau_2) \sum_{n=1}^{\infty} \langle B_n \rangle^2 \times \frac{n \Delta f_B}{\pi} \frac{1}{(n \Delta f_B)^2 + (f - n \langle f_B \rangle)^2}, \quad (27)$$

where $\langle P(f) \rangle_{\rm ave}$ is the averaged power density spectrum defined in § IV,

$$g(m, \tau_1, \tau_2) = K \int_{\tau_1}^{\tau_2} \tau^{-(m-2)} d\tau, \quad (28)$$

and Δf_B is the width of the beat-frequency distribution. This spectrum is displayed graphically in Figure 10, for the wave form of equation (13), with $\langle N \rangle = 100$ and $\eta = 0.035$.

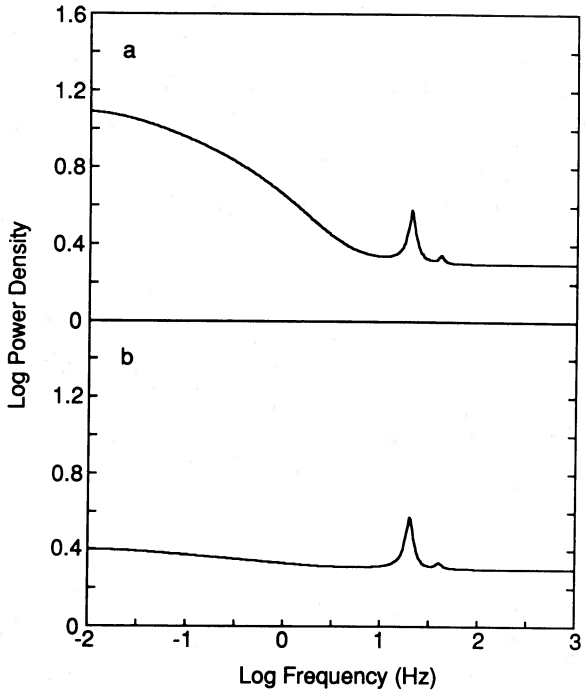

FIG. 10.—Model power spectra showing the effects of pulse-to-pulse correlations in the phases of the oscillating components of the pulses. (*a*) No correlations, $\Delta f_B = 0.8$ Hz, $2\nu \langle A^2 \rangle / \langle I \rangle = 400$. (*b*) Correlation coefficient $\eta\nu = 35$, $\Delta f_B = 2$ Hz, $\langle A^2 \rangle = \langle A \rangle^2$, $2\nu \langle A^2 \rangle / \langle I \rangle = 20$. Both curves assume an exponential envelope function, the modulation function of eq. (10) with $q = 3$, the Lorentzian beat-frequency distribution (11) with $\langle f_B \rangle = 20$ Hz, and the power-law lifetime distribution (12) with $\tau_1 = 0.05$ s, $\tau_2 = 10$ s, and $m = 3$.

VIII. DISCUSSION

The beat-frequency modulated-accretion (BFMA) model of quasi-periodic oscillations in luminous X-ray stars appears especially attractive at present for the reasons summarized in § I. Several new observational results provide additional support for the model (see also Brainerd, Lamb, and Shibazaki 1987). Evidence that the QPO photons in Cyg X-2 and GX 5−1 are harder than typical photons emitted by these sources (Hasinger 1986*b*; van der Klis 1986) supports the prediction of the BFMA model that the QPOs are oscillations in the emission from the neutron star, which is expected to have a relatively hard spectrum, rather than in the emission from the disk, which is expected to have a softer spectrum. Evidence that the QPO photons from Cyg X-2 are comptonized by passing through a scattering cloud of optical depth ~3–15 and radius ~100 km (Hasinger 1986*b*) supports earlier theoretical arguments based in part on the BFMA model (Lamb 1986; see also Paper I) that the neutron star and magnetosphere are immersed in a central scattering cloud of this optical depth and radius. Similar evidence of comptonization has recently been reported in GX 5−1 (van der Klis 1987). Such a cloud strongly suppresses pulsations at the stellar spin frequency without significantly affecting QPOs produced, as in the BFMA model, by modulation of the stellar luminosity (see Paper I; Lamb 1986; Brainerd and Lamb 1987; Brainerd, Lamb, and Shibazaki 1987). Thus, while detection of weak pulsations at the spin frequency remains a key observation that would confirm the BFMA model, there is now direct observational evidence for the presence of a central scattering cloud that explains the weakness of such pulsations.

As noted in § I, at high accretion rates the beat frequency model quantitatively reproduces (see Paper I) the strong positive correlation of QPO frequency with total ~1–20 keV X-ray intensity observed in GX 5−1 (van der Klis *et al.* 1985*b*) and Cyg X-2 (Hasinger *et al.* 1986). However, in Sco X-1 the QPO frequency shows a strong positive correlation with intensity at some times but a weak negative correlation at others (Middleditch and Priedhorsky 1986; van der Klis and Jansen 1986; Priedhorsky *et al.* 1986; van der Klis *et al.* 1985*c*, 1986). This second branch of the frequency-intensity curve can be explained naturally within the beat-frequency model if the accretion rate in Sco X-1 continues to decrease on the negative correlation branch (Priedhorsky 1986). As shown by Ghosh and Lamb (1979; see their Fig. 4), at low mass accretion rates the inner disk is heated by energy pumped into the disk by magnetic stresses. In accretion-powered pulsars this heating

contributes at most a few percent of the luminosity of the system, since the radius of the magnetosphere is ~20–100 times the radius of the star. In the beat frequency model of QPOs, on the other hand, this heating can contribute a luminosity comparable to that of the system, since the radius of the magnetosphere is typically only a few times the radius of the star. In this interpretation, the QPO frequency continues to decrease with decreasing mass flux as predicted by the BFMA model; at high accretion rates the accretion luminosity dominates the total luminosity, which therefore decreases with decreasing mass flux, but as the accretion rate becomes lower the luminosity eventually increases slightly due to the energy supplied by the rotation of the star, creating the second (negative correlation) branch of the frequency-intensity curve.

In the present section we first summarize the key results obtained in our theoretical study of QPO power-density spectra and then compare these results with the observational data on QPO power spectra available at present.

a) Summary of Theoretical Results

Pulse wave form.—The duration of the X-ray pulse, which is described by the envelope function, affects the shape of the red-noise component of the power spectrum and the width of any incoherent oscillation peaks. For pulses lasting a time τ, the red-noise power density rises with decreasing frequency down to $f \approx 1/2\pi\tau$ and then flattens (see Fig. 3). The finite lifetimes of the pulses also contribute a partial width $\Delta f_L \approx 1/2\pi\tau$ to the total widths of any incoherent oscillation peaks in the power spectrum but do not contribute to the widths of any coherent peaks. The lifetimes of the pulses also affect the total power in the red noise and the oscillations, which both scale as τ^2 for constant $2\langle A^2\rangle\nu/\langle I\rangle$. For a given modulation function, the shape of the envelope function has a weak effect on the *total* power in the red noise and the oscillations but does not affect the *ratio* of the total power in the red noise to that in the oscillations.

Overtones of the beat frequency may appear in the modulation function for two reasons. First, a fluctuation orbiting the magnetosphere may produce more than one maximum and minimum in the X-ray intensity per circuit. Second, the variation of the X-ray intensity with the stellar azimuth of the fluctuation may not be sinusoidal. There is a possibility of observationally distinguishing between these two causes of overtones, since a nonsinusoidal variation in intensity with fluctuation azimuth produces a spectrum in which higher overtones are progressively weaker, whereas if a fluctuation produces more than one maximum or minimum per circuit, the power in one or more overtones may exceed that in the fundamental.

For a given envelope function, both the mean value of the modulation function and its harmonic content strongly affect the ratio of the total power in the red noise to that in the peak at the fundamental oscillation frequency. The power in the red noise is proportional to the square of the mean value of the pulse, whereas the power in the oscillations is independent of the mean value. Thus if the mean value is very small, the total power in the red noise can be small compared to that in the oscillations. However, this requires a "finely tuned" pulse wave form and therefore appears unlikely.

Even if the mean value is not small, for sufficiently sharply peaked oscillations in the pulse wave form the total power in the fundamental oscillation peak can exceed that in the red noise (see Fig. 3). However, a strong fundamental oscillation produced by this effect is necessarily accompanied by significant power in overtones. Moreover, as the power in the fundamental peak increases relative to that in the red noise, the strengths of the overtones relative to the fundamental increase rapidly (see Table 2). Changes in the mean value or harmonic content of the pulses can change the red noise to fundamental oscillation power ratio even without changes in other properties of the source.

Fluctuation lifetime distribution.—The distribution of the lifetimes of the density and magnetic-field fluctuations in the boundary layer (and hence the durations of the X-ray pulses they produce) affects both the spectrum of the red-noise component and the shape of any incoherent QPO peaks in the power spectrum.

As noted above, if the distribution of fluctuation lifetimes is narrow (all fluctuations have approximately the same lifetime τ) the red-noise power density rises with decreasing frequency down to $f \approx 1/2\pi\tau$ and then flattens. For an exponential envelope, the power in the red noise above $1/2\pi\tau$ is about half the total power in the red noise and hence approximately equal to the power in a single incoherent oscillation peak. If instead the distribution of fluctuation lifetimes is broad, the red-noise spectrum can continue to rise smoothly down to frequencies comparable to the inverse lifetime of the longest-lived fluctuations (see Figs. 4 and 5). Moreover, if the mean fluctuation lifetime greatly exceeds $1/2\pi f_p$, much of the power in the red noise is shifted to frequencies small compared to f_p.

As a result of this shift of power density to low frequencies, a broad lifetime distribution in which most of the lifetimes are long can make the *apparent* total power in the red noise appear small, even though the *actual* total power in the red noise is relatively large. For example, if $f_p = 20$ Hz and most fluctuations live ~10 s, the red-noise power above 2 Hz ($= 0.1f_p$) is only ~1% of the power in the oscillations while that above 0.2 Hz ($= 0.01f_p$) is still only ~10% of the power in the oscillations. Obviously, changes in the distribution of fluctuation lifetimes can change the total observed power in the red noise relative to that in the oscillations dramatically without changing other properties of the source.

Although the distribution of fluctuation lifetimes affects the shape of any incoherent oscillation peaks in the power spectrum, this effect is much less dramatic than the effect on the red-noise spectrum. The distribution of fluctuation lifetimes has no effect on the shape of any coherent peaks. Thus, *the shape of the red-noise component of the spectrum provides the most direct evidence concerning the lifetime distribution.*

Orbital frequency distribution.—The distribution of the orbital frequencies of the fluctuations in the boundary layer affects the shapes of both incoherent and coherent oscillation peaks but not the shape of the red-noise component. A spread Δf_c in the orbital frequencies causes a spread Δf_B in the beat frequencies of the fluctuations, which contributes a partial width $n\Delta f_B$ to the total width of the peak at the nth harmonic (see Fig. 6). As noted in § IV, one physical cause of a spread in orbital frequencies is that fluctuations may form at different radii in the boundary layer, where the angular velocity of the circulating flow is different. The effect on the power spectrum of the spread in the radii at which the fluctuations orbit within the boundary layer can be described accurately by a distribution of beat frequencies that reflects the radial distribution of the fluctuations.

Another physical cause of a spread in orbital frequencies is the inward drift of density fluctuations that enter the boundary

layer or form within it. As a result of this drift, the radius and hence the beat frequency of each fluctuation changes with time. This frequency modulation of the pulse wave form causes wiggles to appear in the wings of the oscillation peaks (see Alpar 1986). For example, if the beat frequency increases linearly with time there are valleys on the high-frequency side of the oscillation peak at the frequencies $f_n = f_p + \Delta f_n$, where $\Delta f_n = (8n\pi\Delta f_B \Delta f_L)^{1/2}$ and $n = 1, 2, 3, \ldots$ is the number of the valley, counting from the center of the peak. For the valleys to occur in the central part of the peak rather than the far wings, and hence to have an amplitude that is an appreciable fraction of height of the main peak, requires $\Delta f_n/\Delta f_B \lesssim 1$ or $\Delta f_B \gtrsim 4\pi n \Delta f_L$. This condition is equivalent to the statement that shear broadening strongly dominates lifetime broadening. Averaging the power spectrum over the actual distribution $\rho(f_B)$ of beat frequencies in the boundary layer does not provide an accurate description of this phenomenon. However, the modulation function (5) can be easily generalized to include this effect.[8]

Nonuniform phase distributions.—If fluctuations enter the boundary layer or form within it more readily at some stellar azimuths than at others, due for example to the variation of the magnetospheric properties with azimuth, this will cause the initial phases of the pulses they produce to be nonuniformly distributed. Such a nonuniform distribution creates interference between the red noise and oscillation Fourier amplitudes, distorting the high-frequency part of the red-noise spectrum and causing the oscillation peak to become asymmetric (see Fig. 7). Because the distortion is caused by interference, it is most pronounced when the pulse duration is so short that the red-noise and oscillation components of the spectrum significantly overlap. For exponential pulses, the power density just below the oscillation peak is suppressed if the phase distribution peaks near $\phi = 0°$ and enhanced if the distribution peaks near $\phi = 180°$.

Since the power density of the red noise is suppressed at frequencies below the oscillation peak if the initial phase distribution peaks near $\phi = 0$, a nonuniform distribution of initial stellar azimuths and hence of initial pulse phases can also alter the ratio of the apparent power in the red noise to that in the oscillations. However, this effect is generally small, as illustrated by Figure 7.

Variations in pulse rate.—Any nonuniformity in the distribution of pulse times, which corresponds to a variation in the pulse rate, increases the power in the red noise. Periodic variation of the pulse rate can cause a peak in the red-noise component of the spectrum that is unrelated to the oscillating wave form of the pulses (see Fig. 8). A peak in the red noise caused by oscillation of the pulse rate can in principle be distinguished from a peak produced by oscillation of the pulse wave forms in several ways. First, the width of the former can be independent of the shape of the red-noise spectrum whereas the width of the latter necessarily depends at least in part on it. Second, a peak in the red noise can only be strong at frequencies where the red noise is strong. Finally, the power of a peak in the red noise is necessarily proportional to the total power in the red noise. Such a peak can only be present when red noise is present.

Pulse-to-pulse correlations.—Any spatial clustering of fluctuations in the boundary layer (see Fig. 2) creates pulse-to-pulse correlations in the phases of the oscillating components of the X-ray pulses produced by the clustered fluctuations. Such clustering may be caused by several mechanisms. For example, interaction of the magnetosphere with persistent regions of enhanced density in the inner disk may cause plasma to enter the boundary layer preferentially at certain azimuths, producing clusters of fluctuations at these azimuths. Such clustering may also occur if fluctuations just outside the boundary layer fragment into many smaller fluctuations which then drift into the boundary layer. Similarly, if the existence of a slight local excess of plasma orbiting in the boundary layer enhances the rate at which plasma in the inner disk enters the boundary layer at the instantaneous azimuth of the excess, excesses can persist, creating clusters of fluctuations. Finally, interaction between fluctuations within the boundary layer may cause them to cluster.

Even a weak spatial correlation can increase the total power in the oscillations relative to that in the red noise by a factor of 10 or more. For example, if there are 100 fluctuations in the boundary layer and 50% of them are divided among seven clusters, so that there are about seven fluctuations in each cluster, and if $\langle B \rangle^2 \approx \langle B^2 \rangle \approx 2\langle A^2 \rangle$, the total power in the QPO peak is ~ 10 times that in the red noise (see Fig. 10). Obviously, variations in the degree of clustering can change the power ratio substantially without changing the other properties of the source.

We stress that although our work has been motivated by the beat-frequency model, our results apply equally well to other physical models that satisfy the assumptions listed at the end of § II*b* and therefore predict X-ray intensity time series that can be represented by the random processes that we have considered.

b) Comparison with Observation

QPO to red-noise power ratio.—In the luminous QPO X-ray sources so far discovered, the total power P_p in the principal oscillation peak is typically comparable to or greater than the total observed power in the red noise, when oscillations are observed. For example, when oscillations are observed in GX 5−1 the total power in the oscillation peak is comparable to the power in the red noise above 0.5 Hz (van der Klis *et al.* 1985*a*, *b*; Elsner *et al.* 1986). In Cyg X-2 the total power in the oscillation peak is also comparable to that in the red noise above 0.5 Hz at the lowest source intensities observed (Hasinger *et al.* 1985, 1986). However, at the highest intensities, it declines to only $\sim 15\%$ of the power in the red noise above 0.5 Hz. The total observed power in the red noise has also been reported to be comparable to that in the oscillation peak in GX 349+2 (Cooke, Stella, and Ponman 1985), GX 3+1 (Lewin *et al.* 1986*a*, *b*), and at times in GX 17+2 (Stella, Parmar, and White 1985).

In Sco X-1, the total power in the red noise above 0.016 Hz is sometimes less than 10% of that in the oscillations (van der Klis and Jansen 1986; Middleditch and Priedhorsky 1986; Priedhorsky *et al.* 1986; van der Klis *et al.* 1985*c*, 1986). The total observed power in the red noise has also been reported to be small at times in GX 17+2 (Langmeier *et al.* 1985) and in the "rapid burster" (Stella *et al.* 1985; Stella 1986). We note that presently available Sco X-1 power spectra are based on data obtained with the *EXOSAT* xenon ME detectors, which are sensitive to photons in the energy range ~ 8–20 keV, an

[8] As noted by Alpar (1986), the spectra shown in his Figs. 2*b* and 2*c*, which illustrate the effect of radial drift, are plotted on a logarithmic scale and do not include the Poissonian noise component of the spectrum; as a result, the wiggles appear much more dramatic than they would if a realistic Poissonian noise power density were included.

energy range different from that used to observe the other sources and on the high-energy tail of the spectrum.

The relative weakness of the red noise in all these sources is significant for any physical model of their X-ray intensity time series that can be modeled by a random process (Paper I; Lamb 1986; see also Elsner *et al.* 1986). As explained in § III, random processes in which the pulses are positive at all times, uncorrelated, and purely sinusoidal produce power spectra in which the total power P_p in the principal oscillation peak is less than half the total power P_{RN} in the red noise. Since spectra of this type do not agree with most of the QPO spectra observed to date, including the original spectra of GX 5−1, one or more of these simplifying assumptions must be discarded in developing random process models of QPOs.

As mentioned in Paper I and considered in more detail in the present paper, apparent or even real QPO to red-noise power ratios comparable to or greater than unity can be caused by a variety of effects. These include (1) a fluctuation lifetime distribution that extends to relatively long lifetimes, which increases the power ratio in the observed frequency range, (2) nonsinusoidal pulse wave forms, (3) pulse-to-pulse correlations, and (4) suppression of the mean value of the pulses. The need for one or more of these effects was already stressed in Paper I. Indeed, both models of the GX 5−1 spectrum presented in Paper I (see Fig. 5 of that paper) have real or apparent power ratios of order unity. In one model, a power ratio of order unity was caused by the shape of the pulse wave form; in the other model, by a distribution of pulse lifetimes that included a significant number of relatively long-lived pulses.

The spectra of Figures 3*b*, 4*c*, and 5*b* in the present work give qualitative agreement with the spectra of GX 5−1 and Cyg X-2 reported by van der Klis *et al.* (1985*b*) and Hasinger *et al.* (1986). The agreement appears particularly good for lifetime distributions that extend to lifetimes ~ 10 s and for shear broadening less than the lifetime broadening. Thus in these sources and others like them, a modestly peaked pulse wave form, a moderately broad distribution of pulse lifetimes, or some combination of these two mechanisms can account for the observed power ratio. Very long fluctuation lifetimes, pulse-to-pulse correlation effects, and interactions between fluctuations and the magnetosphere that suppress the mean values of pulses may be present but are not required.

It does not appear possible to account for the power ratios as large as 10 to 1 reported in Sco X-1 (Priedhorsky *et al.* 1986; van der Klis *et al.* 1986) and some other sources solely by a peaked pulse wave form. Power ratios this large may be explained if most fluctuations persist as long as 60 s, or if some mechanism "tunes" fluctuations in the boundary layer so that the *mean* intensity of the pulses they produce is reduced by a factor of 3 or more. Perhaps a promising explanation is that there are persistent density variations in the inner disks of these sources (see, for example, Zurek and Benz 1986) or relatively few large fluctuations that fragment as they enter the boundary layer, contributing a few clusters of fluctuations to a much larger number of fluctuations that are not clustered. For example, Figure 10 shows what happens when seven larger fluctuations form seven clusters of about seven fragments each; 50 other fluctuations are assumed to be randomly distributed making a total of 100 fluctuations in the boundary layer. This spectrum agrees qualitatively with the spectra of Sco X-1 reported by Priedhorsky *et al.* (1986) and van der Klis *et al.* (1986). Note the strong enhancement of the QPO peak relative to the red noise (in this example, the power in the QPO peak is ~ 10 times that in the red noise). The width of the peak can be much less than the characteristic width ($\sim \langle 1/2\pi\tau \rangle$) of the red-noise spectrum. If the percentage of fluctuations in clusters is larger or the number of clusters smaller, the increase in the power in the oscillations is still greater.

Despite the fact that the significance of the strength of the oscillations in GX 5−1 and Cyg X-2 was already stressed in Paper I and examples of BFMA models that agree qualitatively with the observations of these sources given there, several authors (Hasinger 1986*a*; van der Klis and Jansen 1986) have mentioned the fact that the QPO power observed in GX 5−1 and Cyg X-2 is sometimes comparable to the red-noise power as a possible difficulty for the BFMA model, based on their assumptions that the pulse wave form is purely sinusoidal, that all pulses have the same lifetime, and that there are no correlations between pulses. In our view, insistence on these assumptions is not supported by the physics of the beat-frequency model. The weaker red noise observed in Sco X-1 has been mentioned by other authors as a possible difficulty (van der Klis *et al.* 1986). In view of the very weak clustering required to account for it, we do not regard it as a serious difficulty at present. We strongly encourage observers to make detailed power spectral observations that have the possibility of detecting the signatures of clustering discussed in § VII.

Changes in power ratio.—At some times spectra of GX 5−1 (van der Klis *et al.* 1985*b*), GX 17+2 (Stella, Parmar, and White 1985), and Sco X-1 (van der Klis *et al.* 1985*c*; Middleditch and Priedhorsky 1986; van der Klis *et al.* 1986) show substantial red noise but no apparent oscillations. Within the BFMA model such spectra could be caused by changes in the structure of the boundary layer that produce a smaller number of fluctuations, if the QPO peak is partially coherent, or reduce the amplitude of the oscillating component of the pulse wave form, or both. Such spectra could also be caused by a decrease in the mean lifetime of fluctuations that shifts red-noise power density to frequencies near the oscillation peak and spreads the oscillation peak over such a broad range of frequencies that it is no longer detectable as a distinct feature.

Despite the fact that Paper I noted several mechanisms by which the power ratio could change in a given source with little or no change in other source properties, some authors (Hasinger 1986*a*; van der Klis and Jansen 1986) have mentioned changes in the power ratio as a potential difficulty for the BFMA model, based on their assumptions that the harmonic content, lifetime distribution, and correlation properties of the pulses remain the same at all times. Again, these simplifying assumptions do not appear to be required by the physics of the BFMA model.

Broad oscillation peaks.—Cooke, Stella, and Ponman (1985) have reported a very broad ($f_p \approx 5$ Hz, $\Delta f_p \approx 15$ Hz) oscillation peak in GX 349+2. In fitting random process models to spectra like this one it is essential to allow for shear as well as lifetime broadening of the oscillation peak.

Structure in oscillation peaks.—A related question is whether there could be observable wiggles in the oscillation peaks of some sources caused by frequency modulation of the pulse wave form. Comparison of the spectra computed in the preceding sections with observed spectra that contain significant red noise indicates that shear broadening is less than or at most of the order of the lifetime broadening and hence that wiggles caused by frequency modulation should be negligible in these

spectra. However, shear broadening may exceed lifetime broadening in spectra in which the red noise is weak, if the weakness is caused by long-lived fluctuations. Thus, spectra with weak apparent red noise may present the best opportunity to observe wiggles in the wings of oscillation peaks. In order to investigate the possible presence of such structure, observations with high-frequency resolution will be required. Even then, relatively small changes in the boundary layer structure over the observing interval could smear out the wiggles, rendering them undetectable.

Possible presence of overtones.—Possible overtones of the fundamental oscillation frequency have been reported in Cyg X-2 (Hasinger 1986*b*), Terzan 2 (Belli *et al.* 1986), and the "rapid burster" (Stella *et al.* 1986). Our calculations show that prominent overtones are to be expected in the beat-frequency model when the interaction of fluctuations with the magnetosphere varies sharply with stellar azimuth.

Appearance of peaks at ~5–6 Hz.—Power spectral peaks at ~5–6 Hz have been reported in Sco X-1 (Middleditch and Priedhorsky 1986; Priedhorsky *et al.* 1986; van der Klis *et al.* 1986), Cyg X-2 (Hasinger 1986*b*; Norris and Wood 1985, 1986), and GX 5−1 (van der Klis 1986). In Sco X-1, the peak at this frequency appears to be the result of a smooth decrease in peak frequency with changes in the X-ray intensity and spectrum and hence is probably caused by the same physical mechanism that produces the peak when it is at higher frequencies.

On the other hand, the peaks occasionally seen at ~5–6 Hz in Cyg X-2 and GX 5−1 appear to be a distinct phenomenon. When observed, these peaks are on the shoulder of the red-noise spectrum. Peaks like these, which appear only when red noise is present and at frequencies where the red noise is strong can be readily produced by variations in the pulse rate, as noted in § VIII*a*. As discussed there, peaks produced by oscillations in the pulse rate can in principle be distinguished from peaks caused by oscillating pulse wave forms by the behavior of their width and by the fact that the total power in such peaks is proportional to the total power in the red noise. We encourage analyses designed to test the hypothesis that these ~5–6 Hz peaks are caused by variations in the pulse rate.

IX. CONCLUSIONS

In the present paper we have considered a variety of partially random processes, in order to study the effects on the power-density spectrum of several physical phenomena that may occur in the beat-frequency model of QPOs. We have shown that the shape of the oscillating component of the X-ray pulse wave form can profoundly affect the strength of the oscillations relative to the red noise as well as the relative strengths of the harmonics of the oscillation frequency. We have also explored the effects on the power spectrum of distributions in the lifetimes and orbital frequencies of the density fluctuations in the boundary layer and shown that the lifetime distribution, especially, can strongly affect the spectrum of the red noise. We have presented closed expressions that include these effects and are suitable for fitting to observed power spectral data. Fragmentation of fluctuations or interaction between fluctuations may cause some spatial clustering. We have shown that even very weak clustering can cause the total power in the oscillations to exceed that in the red noise by one order of magnitude or more. Changes in the wave forms of pulses, the lifetimes of fluctuations, and the degree of clustering can produce a complicated relation between the strength of the red noise and that of the oscillations.

We have also considered some simple models that illustrate the effects on the power spectrum of nonuniform distributions of the initial stellar azimuths and times of the density fluctuations, which could be caused by their interaction with the magnetospheric field and plasma. We have shown that variations in the rate of formation of density fluctuations can cause a peak in the red-noise component of the power spectrum. A peak formed in this way can only be present when red noise is present and is strongest and hence most readily observed at the frequencies where the red noise is strongest.

We have compared our theoretical power density spectra with currently available observed spectra of 5–50 Hz QPOs in luminous X-ray sources. The theoretical spectra are in qualitative agreement with observed spectra, including those obtained in recent observations. Recent X-ray spectral observations which show that the QPO photons in Cyg X-2 and GX 5−1 are harder than typical photons support the beat-frequency modulated-accretion model. Recent direct evidence for central scattering clouds in Cyg X-2 and GX 5−1, of the size and optical depth suggested earlier on the basis of the beat-frequency model, provides additional support. We conclude that the beat-frequency model remains highly promising. Detection of weak pulsations at the neutron star spin frequency remains a key observation that would confirm this model.

Although motivated by the beat-frequency model, our power spectral models have much wider applicability since, as pointed out by Lamb (1986), random processes can also be used to describe the X-ray intensity time series predicted by a variety of other QPO models. Therefore, *we encourage observers to fit these models to their data and report the resulting parameters as a compact and physically meaningful way of summarizing observations.* Reporting observations in this way would make it much easier to compare observations of different sources and different observations of the same source. Obviously, the results of such fits can also be used to constrain physical models.

It is a pleasure to thank R. Elsner, M. van der Klis, W. Priedhorsky, and M. Weisskopf for helpful comments. We also thank V. Petrosian, P. Sturrock, and R. Wagoner for their warm hospitality at Stanford University while this work was being completed. F. K. L. also thanks the John Simon Guggenheim Memorial Foundation for generous support. This research was supported in part by NASA grants NSG 7653 (at Illinois) and NGR 05-020-668 and NAGW 299 (at Stanford) and by NSF grants PHY 80-25605 and PHY 86-0037 (at Illinois) and PHY 81-18387 and PHY 86-03273 (at Stanford).

APPENDIX

AVERAGING OVER FREQUENCY AND LIFETIME DISTRIBUTIONS

In this appendix we summarize the steps involved in averaging the reference spectrum (6) over the frequency and lifetime distributions (11) and (12).

The full expression for the power-density spectrum averaged over the frequency and lifetime distributions may be obtained by replacing the function $|S(f \pm nf_B)|^2$ in equation (6) by the averaged function $\langle |S(f \pm nf_B)|^2 \rangle_{\rm ave}$. As explained in § IV, for simplicity we assume an exponential envelope function. Then $|S(f)|^2$ has the Lorentzian form shown in Table 1. It is convenient to first average $|S(f)|^2$ over the beat-frequency distribution (11), since the result may be written as a single expression, namely,

$$\int_0^\infty \rho(f_B)|S(f \pm nf_B)|^2 df_B = \frac{(1 + 2\pi n\Delta f_B \tau)}{[2\pi(f \pm n\langle f_B\rangle)]^2 + (\tau^{-1} + 2\pi n\Delta f_B)^2} . \tag{A1}$$

Next, we average the result (A1) over the lifetime distribution (eq. [12]). Different expressions result, depending on the value of the power-law index m in the distribution. Here we give expressions corresponding to $m = 1, 2, 3$, and 4.

$m = 1$:

$$\langle |S(f \pm nf_B)|^2 \rangle_{\rm ave} = \int_0^\infty \int_{\tau_1}^{\tau_2} \rho(f_B)\rho(\tau)|S(f \pm nf_B)|^2 df_B\, d\tau$$

$$= K\left\{\left[\frac{0.5}{D} - \left(\frac{n\Delta\omega_B}{D}\right)^2\right]\left(Q + 2\ln\frac{\tau_2}{\tau_1}\right) - \frac{n\Delta\omega_B}{D}(\tau_1 - \tau_2) + \frac{n\Delta\omega_B}{D}\left[-1 + \frac{(n\Delta\omega_B)^2 - (\omega \pm n\langle\omega_B\rangle)^2}{D}\right]U\right\}, \tag{A2}$$

where $K = 1/\ln(\tau_2/\tau_1)$, $\omega = 2\pi f$, $\langle\omega_B\rangle = 2\pi\langle f_B\rangle$, and $\Delta\omega_B = 2\pi\Delta f_B$,

$$D = (\omega \pm n\langle\omega_B\rangle)^2 + (n\Delta\omega_B)^2 , \tag{A3}$$

$$Q = \ln\left[\frac{(\omega \pm n\langle\omega_B\rangle)^2 + (\tau_2^{-1} + n\Delta\omega_B)^2}{(\omega \pm n\langle\omega_B\rangle)^2 + (\tau_1^{-1} + n\Delta\omega_B)^2}\right], \tag{A4}$$

and

$$U = \frac{1}{\omega \pm n\langle\omega_B\rangle}\left[\tan^{-1}\left(\frac{\tau_1^{-1} + n\Delta\omega_B}{\omega \pm n\langle\omega_B\rangle}\right) - \tan^{-1}\left(\frac{\tau_2^{-1} + n\Delta\omega_B}{\omega \pm n\langle\omega_B\rangle}\right)\right]. \tag{A5}$$

Note that $U \to 0$ as $\omega \to -n\langle\omega_B\rangle$ (for plus signs in expression [A5]) and $+n\langle\omega_B\rangle$ (for minus signs in expression [A5]).

$m = 2$:

$$\langle |S(f \pm nf_B)^2| \rangle_{\rm ave} = K\left\{\frac{n\Delta\omega_B}{2D}\left[Q + 2\ln\left(\frac{\tau_2}{\tau_1}\right)\right] + \left[1 - \frac{(n\Delta\omega_B)^2}{D}\right]U\right\} \tag{A6}$$

where now $K = \tau_1\tau_2/(\tau_2 - \tau_1)$.

$m = 3$:

$$\langle |S(f \pm nf_B)|^2 \rangle_{\rm ave} = \frac{KQ}{2} , \tag{A7}$$

where $K = 2(\tau_1\tau_2)^2/(\tau_2^2 - \tau_1^2)$.

$m = 4$:

$$\langle |S(f \pm nf_B)|^2 \rangle_{\rm ave} = K\left[(\tau_1^{-1} - \tau_2^{-1}) - \frac{n\Delta\omega_B}{2} Q - (\omega \pm n\langle\omega_B\rangle)^2 U\right], \tag{A8}$$

where $K = 3/(1/\tau_1^3 - 1/\tau_2^3)$.

REFERENCES

Alpar, M. A. 1986, *M.N.R.A.S.*, **223**, 496.
Alpar, M. A., and Shaham, J. 1985, *Nature*, **316**, 239.
Belli, B. M., d'Antona, F., Molteni, D., and Morini, M. 1986, *IAU Circ.*, No. 4174.
Boyle, C. B., Fabian, A. C., and Guilbert, P. W. 1986, *Nature*, **319**, 648.
Brainerd, J., and Lamb, F. K. 1987, *Ap. J. (Letters)*, **317**, L33.
Brainerd, J., Lamb, F. K., and Shibazaki, N. 1987, in *Proc. 13th Texas Symposium on Relativisitic Astrophysics* (World Scientific Publishers), in press.
Cooke, B. A., Stella, L., and Ponman, T. 1985, *IAU Circ.*, No. 4116.
Cordova, F. A., and Mason, K. O. 1983, in *Accretion-Driven Stellar X-Ray Sources*, ed. W. H. G. Lewin and E. P. J. van den Heuvel (Cambridge: Cambridge University Press), p. 147.
Elsner, R. F., Weisskopf, M. C., Darbo, W., Ramsey, B. D., Williams, A. C., Sutherland, P. G., and Grindlay, J. E. 1986, *Ap. J.*, **308**, 655.
Ghosh, P., and Lamb, F. K. 1979, *Ap. J.*, **232**, 259.
Hameury, J. M., King, A. R., and Lasota, J. P. 1985, *Nature*, **317**, 597.
Hasinger, G. 1986*a*, in *The Evolution of Galactic X-Ray Binaries*, ed. J. Trümper, W. H. G. Lewin, and W. Brinkmann (Dordrecht: Reidel), p. 139.
———. 1986*b*, in *IAU Symposium 125, The Origin and Evolution of Neutron Stars*, ed. D. J. Helfand and J. H. Huang (Dordrecht: Reidel), in press.
Hasinger, G., Langmeier, A., Sztajno, M., and Pietsch, W. 1985, *IAU Circ.*, No. 4153.
Hasinger, G., Langmeier, A., Sztajno, M., Trümper, J., Lewin, W. H. G., and White, N. E. 1986, *Nature*, **319**, 469.
Joss, P. C., Avni, Y., and Rappaport, S. 1978, *Ap. J.*, **221**, 645.
Lamb, F. K. 1986, in *The Evolution of Galactic X-Ray Binaries*, ed. J. Trümper, W. H. G. Lewin, and W. Brinkmann (Dordrecht: Reidel), p. 151.

Lamb, F. K., Shibazaki, N., Alpar, M. A., and Shaham, J. 1985, *Nature*, **317**, 681 (Paper I).
Langmeier, A., Hasinger, G., Sztajno, M., Trümper, J., and Pietsch, W. 1985, *IAU Circ.*, No. 4147.
Leahy, D. A., *et al.* 1983, *Ap. J.*, **266**, 160.
Lewin, W. H. G., *et al.* 1986*a*, *IAU Circ.*, No. 4170.
———. 1986*b*, *M.N.R.A.S.*, submitted.
Lewin, W. H. G., van Paradijs, J., Jansen, F., van der Klis, M., Sztajno, M., and Trümper, J. 1985, *IAU Circ.*, No. 4101.
Li, F. K., Joss, P. C., McClintock, J. E., Rappaport, S., and Wright, E. L. 1980, *Ap. J.*, **240**, 628.
Middleditch, J., and Priedhorsky, W. 1986, *Ap. J.*, **306**, 230.
Morfill, G., and Trümper, J. 1986, in *The Evolution of Galactic X-Ray Binaries*, ed. J. Trümper, W. H. G. Lewin, and W. Brinkmann (Dordrecht: Reidel), p. 173.
Norris, J. P., and Wood, K. S. 1985, *IAU Circ.*, No. 4087.
———. 1987, *Ap. J.*, **312**, 732.
Patterson, J. 1979, *Ap. J.*, **234**, 978.
Priedhorsky, W. 1986, *Ap. J. (Letters)*, **306**, L97.
Priedhorsky, W., Hasinger, G., Lewin, W. H. G., Middleditch, J., Parmar, A., Stella, L., and White, N. 1986, *Ap. J. (Letters)*, **306**, L91.
Rice, S. O. 1954, in *Selected Papers on Stochastic Processes*, ed. N. Wax (London: Dover), p. 133.
Scargle, J. D. 1981, *Ap. J. Suppl.*, **45**, 1.
Stella, L. 1986, in *Proc. Mediterranean School on Plasma Astrophysics*, Crete, 1985 September 23–October 4, in press.
Stella, L., Haberl, F., Parmar, A., White, N., Lewin, W. H. G., and van Paradijs, J. 1987, *Ap. J.*, submitted.
Stella, L., Parmar, A. N., and White, N. E. 1985, *IAU Circ.* No. 4102.
———. 1987, *Ap. J.*, submitted.
Stella, L., Parmar, A. N., White, N. E., Lewin, W. H. G., and van Paradijs, J. 1985, *IAU Circ.*, No. 4110.
Stella, L., White, N. E., and Priedhorsky, W. 1985, *IAU Circ.*, No. 4117.
———. 1987, *Ap. J. (Letters)*, in press.
Tenant, A. F. 1987, *M.N.R.A.S.*, submitted.
Tawara, Y., Hayakawa, S., Kunieda, H., Makino, F., Nagase, F. 1982, *Nature*, **299**, 38.
van der Klis, M. 1986, in *Accretion onto Compact Objects, Proc. Tenerife Workshop*, 1986 April 21–25, in press.
———. 1987, in *Proc. Conf. on Variability in Galactic and Extragalactic X-Ray Sources*, Como, Italy, 1986 October, in press.
van der Klis, M., and Jansen, F. 1985, *Nature*, **313**, 768.
———. 1986, in *The Evolution of Galactic X-Ray Binaries*, ed. J. Trümper, W. H. G. Lewin, and W. Brinkmann (Dordrecht: Reidel), p. 129.
van der Klis, M., Jansen, F., van Paradijs, J., Lewin, W. H. G., Trümper, J., and Sztajno, M. 1985*a*, *IAU Circ.*, No. 4140.
van der Klis, M., Jansen, F., van Paradijs, J., Lewin, W. H. G., van den Heuvel, E. P. J., Trümper, J., and Sztajno, M. 1985*b*, *Nature*, **316**, 225.
van der Klis, M., Jansen, F., White, N., Stella, L., and Peacock, A. 1985*c*, *IAU Circ.*, No. 4068.
van der Klis, M., Stella, L., White, N., Jansen, F., and Parmer, A. N. 1986, *Ap. J.*, **316**, 411.
van Paradijs, J., *et al.* 1987, *IAU Circ.*, No. 4308.
Zurek, W. H., and Benz, W. 1986, *Ap. J.*, **308**, 123.

F. K. Lamb: Department of Physics, University of Illinois at Urbana-Champaign, 1110 W. Green Street, Urbana, IL 61801

N. Shibazaki: Space Science Laboratory ES 65, NASA/Marshall Space Flight Center, Huntsville, AL 35812